The *Caenorhabditis elegans* SMOC-1 Protein Acts Cell Nonautonomously To Promote Bone Morphogenetic Protein Signaling

Melisa S. DeGroot, Herong Shi, Alice Eastman, Alexandra N. McKillop, and Jun Liu[1]
Department of Molecular Biology and Genetics, Cornell University, Ithaca, New York 14853
ORCID ID: 0000-0001-7815-4075 (J.L.)

ABSTRACT Bone morphogenetic protein (BMP) signaling regulates many different developmental and homeostatic processes in metazoans. The BMP pathway is conserved in *Caenorhabditis elegans*, and is known to regulate body size and mesoderm development. We have identified the *C. elegans smoc-1* (Secreted MOdular Calcium-binding protein-1) gene as a new player in the BMP pathway. *smoc-1(0)* mutants have a small body size, while overexpression of *smoc-1* leads to a long body size and increased expression of the RAD-SMAD (reporter acting downstream of SMAD) BMP reporter, suggesting that SMOC-1 acts as a positive modulator of BMP signaling. Using double-mutant analysis, we showed that SMOC-1 antagonizes the function of the glypican LON-2 and acts through the BMP ligand DBL-1 to regulate BMP signaling. Moreover, SMOC-1 appears to specifically regulate BMP signaling without significant involvement in a TGFβ-like pathway that regulates dauer development. We found that *smoc-1* is expressed in multiple tissues, including cells of the pharynx, intestine, and posterior hypodermis, and that the expression of *smoc-1* in the intestine is positively regulated by BMP signaling. We further established that SMOC-1 functions cell nonautonomously to regulate body size. Human SMOC1 and SMOC2 can each partially rescue the *smoc-1(0)* mutant phenotype, suggesting that SMOC-1's function in modulating BMP signaling is evolutionarily conserved. Together, our findings highlight a conserved role of SMOC proteins in modulating BMP signaling in metazoans.

KEYWORDS BMP; SMOC-1; SPARC; LON-2; glypican; body size

BONE morphogenetic proteins (BMPs) are highly conserved signaling molecules that mediate cell-to-cell communication. The BMP signaling cascade is initiated when the BMP ligands bind to the membrane-bound receptor kinases, upon which the type II receptor phosphorylates the type I receptors. The signaling cascade is then transduced within the receiving cell as the receptor-associated Smads (R-Smads) are activated via phosphorylation by the type I receptor. Activated R-Smads complex together with common mediator Smads (co-Smads) and other transcription factors to regulate the transcription of downstream genes (Katagiri and Watabe 2016). BMPs regulate fundamental cellular processes, including cell migration, cell proliferation, cell fate specification, and cell death throughout metazoan development (Wang *et al.* 2014). Tight regulation of BMP signaling in time, space, magnitude, and duration is therefore important for proper developmental outcomes. Misregulation of BMP signaling can cause a variety of disorders in humans (Brazil *et al.* 2015; Salazar *et al.* 2016; Wu *et al.* 2016). Previous studies have demonstrated that BMP signaling can be regulated at many levels, both extracellularly and intracellularly (Bragdon *et al.* 2011; Lowery *et al.* 2016; Sedlmeier and Sleeman 2017). The nematode *Caenorhabditis elegans* provides a useful system for identifying factors that modulate the BMP pathway.

The BMP pathway in *C. elegans* is comprised of evolutionarily conserved core components including the ligand (DBL-1/BMP), the type I and type II receptors (SMA-6/RI and DAF-4/RII), the R-Smads (SMA-2 and SMA-3), and the co-Smad (SMA-4) (Estevez *et al.* 1993; Savage *et al.* 1996; Krishna *et al.* 1999; Morita *et al.* 1999, 2002; Suzuki *et al.* 1999) (Figure 1A). Unlike in *Drosophila* and vertebrates, BMP signaling is not essential for viability in *C. elegans*, yet it

doi: https://doi.org/10.1534/genetics.118.301805
Manuscript received August 26, 2018; accepted for publication December 4, 2018; published Early Online December 5, 2018.
[1]Corresponding author: Department of Molecular Biology and Genetics, 439 Biotechnology Bldg., Cornell University, Ithaca, NY 14853. E-mail: JL53@cornell.edu

regulates multiple processes, including body size, male tail development, and mesoderm patterning (Gumienny and Savage-Dunn 2013; Savage-Dunn and Padgett 2017). The BMP ligand DBL-1 is expressed in the ventral nerve cord (Suzuki *et al.* 1999) and it activates the pathway in the hypodermis to regulate body size (Yoshida *et al.* 2001; Wang *et al.* 2002). Reduced BMP signaling causes a small (Sma) body size, while increased BMP signaling leads to a long (Lon) body size (Morita *et al.* 1999, 2002; Suzuki *et al.* 1999). BMP signaling also regulates the development of the postembryonic mesoderm lineage, the M lineage. We have shown that mutations in the BMP pathway specifically suppress the M-lineage dorsoventral patterning defects caused by mutations in *sma-9*, which encodes the *C. elegans* zinc finger protein Schnurri (Liang *et al.* 2003; Foehr *et al.* 2006). Specifically, mutations in *sma-9* result in the loss of the two M-derived coelomocytes (CCs), while BMP pathway mutations can restore these two CCs in the *sma-9(0)* mutant background (Foehr *et al.* 2006; Liu *et al.* 2015; Wang *et al.* 2017) (Figure 1, B and C). Using this suppression of *sma-9(0)* M-lineage defect (Susm) assay, we have identified multiple evolutionarily conserved modulators of BMP signaling. These include the RGM (repulsive guidance molecule) protein DRAG-1 (Tian *et al.* 2010), the neogenin homolog UNC-40 (Tian *et al.* 2013), the ADAM10 protein SUP-17 (Wang *et al.* 2017), and three tetraspanins, TSP-21, TSP-12, and TSP-14 (Liu *et al.* 2015; Wang *et al.* 2017).

In this study, we report the identification and characterization of a new BMP modulator, which we have named SMOC-1 (Secreted MOdular Calcium-binding protein-1). SMOC-1 is predicted to be a secreted protein that contains a thyroglobulin-like (TY) domain and an extracellular calcium (EC)-binding motif. We show here that SMOC-1 acts as a positive modulator of BMP signaling in *C. elegans*. We further demonstrate that SMOC-1 acts genetically upstream of the BMP ligand and functions in a positive feedback loop to promote BMP signaling in regulating body size. We identified *smoc-1*-expressing cells, and demonstrated that SMOC-1 acts cell nonautonomously to regulate BMP signaling. Finally, we provide evidence that the function of SMOC proteins in the BMP pathway is conserved from worms to humans.

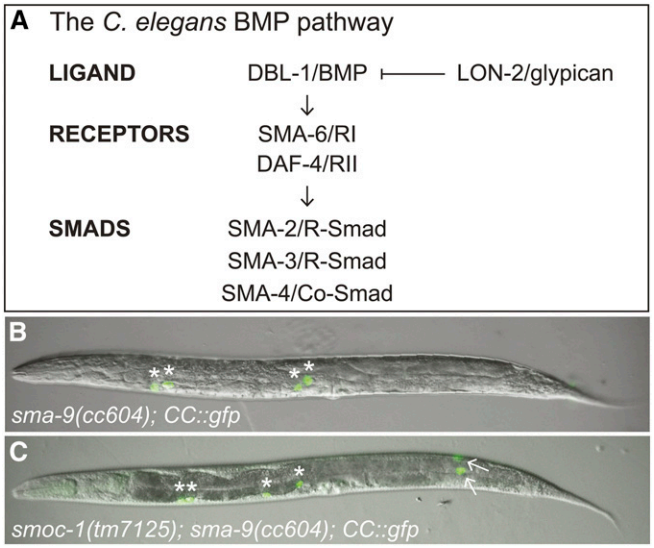

Figure 1 *smoc-1(0)* mutations suppress the *sma-9(0)* M-lineage defect. (A) Schematic representation of the BMP signaling pathway in *C. elegans*. (B and C) Merged DIC and GFP images of L4 stage *sma-9(cc604)* (B) and *smoc-1(tm7125)*; *sma-9(cc604)* (C) worms carrying the *CC::gfp* CC marker. Arrows indicate M-derived CCs. Asterisks (*) denote embryonically-derived CCs. BMP, bone morphogenetic protein; CC, coelomocyte; RI, type I receptor; RII, type II receptor; R-Smad, receptor-regulated Smad; Co-Smad, common mediator Smad.

Materials and Methods

C. elegans strains

All strains were maintained at 20°C using standard culture conditions (Brenner 1974) unless otherwise specified. Table 1 lists all the strains used in this study.

Plasmid constructs and transgenic lines

All plasmid constructs used in this study are listed in Table 2. The *smoc-1* open reading frame was amplified from the Vidal RNA interference library (Rual *et al.* 2004). Subsequent sequencing of the clone revealed the presence of a point mutation (S103P, Figure 2D), changing amino acid 103 from serine (TCC) to proline (CCC). Site-directed mutagenesis was used to fix this point mutation. Plasmids containing the human *SMOC1* and *SMOC2* cDNAs were purchased from PlasmID, the DNA resource core at Harvard Medical School.

Transgenic strains were generated using the plasmids pRF4 *(rol-6(su1006))*, pCFJ90 (*myo-2p*::*mCherry*::*unc-54 3'UTR)*, or pJKL724 (*myo-3p*::*mCherry*::*unc-54 3′ UTR)* as co-injection markers. Two transgenic lines with the best transmission efficiencies were analyzed for each plasmid of interest. Integrated transgenic lines either overexpressing *smoc-1* (*jjIs5119*) or carrying the *smoc-1* transcriptional reporter (*jjIs4688* and *jjIs4694*) were generated using γ-irradiation, followed by three rounds of outcrossing with N2 worms.

Protein sequence alignment

Sequences were taken from GenBank [*C. elegans* SMOC-1 (T04F3.2), 179609; *C. remanei* CRE_26999, 9815068; *C. briggsae* CBG23276, 8578577; *Drosophila melanogaster* Pent/Magu, 44850; *Homo sapiens* SMOC1, 64093; and *H. sapiens* SMOC2, 64094] or WormBase (*C. brenneri* CBN20462, *C. japonica* CJA07338, and *Pristionchus pacificus* PPA34808). TY and EC domains in SMOC proteins were predicted by Interpro (Finn *et al.* 2017). Domains were aligned using the M-COFFEE Multiple Sequence Alignment tool on the T-COFFEE server (version 11.00.d625267; Wallace *et al.* 2006). ALN files were processed to produce alignment images using BOXSHADE.

Microscopy

Epifluorescence and differential interference contrast (DIC) microscopy were conducted on a Leica DMRA2 compound microscope equipped with a Hamamatsu Orca-ER camera

Table 1 Strains used in this study

Strain identifier	Genotype
Original *sma-9* suppressor strains from the EMS screen	
LW0040	*arIs37[secreted CC::gfp] I*; *cup-5(ar465) III*; *sma-9(cc604) X*
LW2697	*arIs37[secreted CC::gfp] I*; *cup-5(ar465) III*; *smoc-1(jj65) V*; *sma-9(cc604) X*
LW2732	*arIs37[secreted CC::gfp] I*; *cup-5(ar465) III*; *smoc-1(jj85) V*; *sma-9(cc604) X*
LW2731	*arIs37[secreted CC::gfp] I*; *sma-4(jj70) cup-5(ar465) III*; *smoc-1(jj180) V*; *sma-9(cc604) X*
LW3874	*arIs37[secreted CC::gfp] I*; *cup-5(ar465) III*; *smoc-1(jj109) V*; *sma-9(cc604) X*
LW3927	*arIs37[secreted CC::gfp] I*; *cup-5(ar465) III*; *smoc-1(jj115) V*; *sma-9(cc604) X*
LW3906	*arIs37[secreted CC::gfp] I*; *cup-5(ar465) III*; *smoc-1(jj139) V*; *sma-9(cc604) X*
Strains with different *smoc-1* alleles	
LW4477	*smoc-1(tm7000) V [6x outcrossed, isolate 3.23]*
LW4478	*smoc-1(tm7000) V [6x outcrossed, isolate 4.5]*
LW4479	*smoc-1(tm7125) V [6x outcrossed, isolate 5.2]*
LW4480	*smoc-1(tm7125) V [6x outcrossed, isolate 7.24]*
LW4766	*smoc-1(jj65) V [5x outcrossed, isolate 2.13]*
LW4487	*smoc-1(jj85) V [3x outcrossed, isolate 1.13]*
LW4555	*smoc-1(jj180) V [5x outcrossed, isolate 5.4]*
LW4556	*smoc-1(jj180) V [5x outcrossed, isolate 5.8]*
LW5623	*smoc-1(jj115) V [3x outcrossed, isolate 3.5]*
LW5624	*smoc-1(jj115) V [3x outcrossed, isolate 13.3]*
LW5129	*jjIs5119[pMSD4.4(smoc-1p::smoc-1 cDNA:: smoc-1 3′UTR)+pCFJ90(myo-2p::mCherry)] I 3x outcrossed, isolate 1.3, also known as smoc-1(OE)*
LW5130	*jjIs5119[pMSD4.4(smoc-1p::smoc-1 cDNA:: smoc-1 3′UTR)+pCFJ90(myo-2p::mCherry)] I 3x outcrossed, isolate 2.5, also known as smoc-1(OE)*
Strains for examining the M-lineage phenotypes of *smoc-1* mutants	
LW0081	*ccIs4438 [intrinsic CC::::gfp] III*; *ayIs2[egl-15p::gfp] IV*; *ayIs6[hlh-8p::gfp] X*
LW4420	*ccIs4438[intrinsic CC::gfp] III*; *ayIs2[egl-15p::gfp] IV*; *smoc-1(tm7000) V*; *ayIs6[hlh-8p::gfp] X*
LW4422	*ccIs4438[intrinsic CC::gfp] III*; *ayIs2[egl-15p::gfp] IV*; *smoc-1(tm7125) V*; *ayIs6[hlh-8p::gfp] X*
LW4442	*arIs37[secreted CC::gfp] I*; *ccIs4438[intrinsic CC::gfp] III*; *ayIs2[egl-15p::gfp] IV*; *smoc-1(tm7125) V*; *sma-9(cc604) ayIs6[hlh-8p::gfp] X*
LW4443	*arIs37[secreted CC::gfp] I*; *ccIs4438[intrinsic CC::gfp] III*; *ayIs2[egl-15p::gfp] IV*; *smoc-1(tm7000) V*; *sma-9(cc604) ayIs6[hlh-8p::gfp] X*
LW4457	*arIs37[secreted CC::gfp] I*; *smoc-1(jj180) V*; *sma-9(cc604) X*
LW4834	*arIs37[secreted CC::gfp] I*; *ccIs4438[intrinsic CC::gfp] III*; *smoc-1(tm7125) V*; *sma-9(cc604) ayIs6[hlh-8p::gfp] X*
Strains carrying the RAD-SMAD reporter	
LW2433	*jjIs2433[pCXT51(5*RLR::deleted pes-10p::gfp) + LiuFD61(mec-7p::rfp)] X, isolate 1, also known as RAD-SMAD reporter*
LW3468	*lon-2(e678) jjIs2433[RAD-SMAD] X*
LW5604	*jjIs5119[smoc-1(OE)] I*; *jjIs2433[RAD-SMAD] X, isolate 1*
LW5605	*jjIs5119[smoc-1(OE)] I*; *jjIs2433[RAD-SMAD] X, isolate 2*
Strains for body size measurement	
LW1856	*sma-6(jj1) II*
LW5498	*sma-3(tm4625) III [4x outcrossed, isolate 8.3]*
LW5499	*sma-3(tm4625) III [4x outcrossed, isolate 8.6]*
LW3346	*sma-3(jj3) III*
LW4774	*dbl-1(ok3749) V*
LW3471	*lon-2(e678) X*
LW4703	*sma-6(jj1) II*; *smoc-1(tm7125) V, isolate 9.3.1*
LW4704	*sma-6(jj1) II*; *smoc-1(tm7125) V, isolate 9.6.1*
LW4590	*sma-3(jj3) III*; *smoc-1(tm7125) V, isolate 13.12*
LW4595	*sma-3(jj3) III*; *smoc-1(tm7125) V, isolate 5.9.5*
LW5344	*dbl-1(ok3749) smoc-1(tm7125) V, isolate 1.1.1*
LW5345	*dbl-1(ok3749) smoc-1(tm7125) V, isolate 4.7.8*
LW4617	*smoc-1(tm7125) V*; *lon-2(e678) X, isolate 6.10.3.6*
LW4618	*smoc-1(tm7125) V*; *lon-2(e678) X, isolate 6.7.3.7*
LW5241	*jjIs5119[smoc-1(OE)] I*; *dbl-1(ok3749) V, isolate 2.17*
LW5263	*jjIs5119[smoc-1(OE)] I*; *dbl-1(ok3749) V, isolate 3.11*
LW5621	*jjIs5119[smoc-1(OE)] I*; *sma-3(tm4625) III, isolate 1.2*
LW5622	*jjIs5119[smoc-1(OE)] I*; *sma-3(tm4625) III, isolate 2.3*
LW5294	*jjIs5119[smoc-1(OE)] I*; *lon-2(e678) X, isolate 5*
LW5295	*jjIs5119[smoc-1(OE)] I*; *lon-2(e678) X, isolate 6*
Strains for assaying the dauer phenotype	
DR40	*daf-1(m40) IV*
DR609	*daf-1(m213) IV*

(continued)

Table 1, *continued*

Strain identifier	Genotype
CB1372	*daf-7(e1372) III*
LW5288	*daf-1(m40) IV*; *smoc-1(tm7125) V isolate 7.11B*
LW5289	*daf-1(m40) IV*; *smoc-1(tm7125) V isolate 16.16B*
LW5286	*daf-1(m213) IV*; *smoc-1(tm7125) V isolate 2.4*
LW5287	*daf-1(m213) IV*; *smoc-1(tm7125) V isolate 2.8*
LW5290	*daf-7(e1372) III*; *smoc-1(tm7125) V isolate 6.12*
LW5306	*daf-7(e1372) III*; *smoc-1(tm7125) V isolate 6.6*
LW5291	*daf-1(m213) IV*; *lon-2(e678) X isolate 2.3*
LW5292	*daf-1(m213) IV*; *lon-2(e678) X isolate 2.4*
LW5293	*daf-7(e1372) III*; *lon-2(e678) X isolate 6*
LW5285	*daf-7(e1372) III*; *lon-2(e678) X isolate 15*
Strains carrying the *smoc-1* reporter constructs	
LW4688	*jjIs4688[pJKL1139.2(smoc-1p::4xnls::gfp::unc-54 3′UTR)+pRF4] I or IV*, *3x outcrossed*, *isolate 13.1*
LW4694	*jjIs4694[pJKL1139.2(smoc-1p::4xnls::gfp::unc-54 3′UTR)+pRF4] V*, *3x outcrossed*, *isolate 19.1*
LW4764	*sma-3(jj3) III*; *jjIs4688[pJKL1139.2(smoc-1p::4xnls::gfp::unc-54 3′UTR)+pRF4] I or IV*, *isolate 3.2*
LW4765	*sma-3(jj3) III*; *jjIs4688[pJKL1139.2(smoc-1p::4xnls::gfp::unc-54 3′UTR)+pRF4] I or IV*, *isolate 9.3*
LW4724	*sma-6(jj1) II*; *jjIs4688[pJKL1139.2(smoc-1p::4xnls::gfp::unc-54 3′UTR)+pRF4] I or IV*, *isolate 11.4.2*
LW4725	*sma-6(jj1) II*; *jjIs4688[pJKL1139.2(smoc-1p::4xnls::gfp::unc-54 3′UTR)+pRF4] I or IV*, *isolate 11.7.2*
LW4728	*jjIs4688[pJKL1139.2(smoc-1p::4xnls::gfp::unc-54 3′UTR)+pRF4] I or IV*; *lon-2(e678)*, *isolate 1.3.1*
LW4729	*jjIs4688[pJKL1139.2(smoc-1p::4xnls::gfp::unc-54 3′UTR)+pRF4] I or IV*; *lon-2(e678)*, *isolate 2.1.2*
LW5520	*jjIs4688[pJKL1139.2(smoc-1p::4xnls::gfp::unc-54 3′UTR)+pRF4] I or IV*; *smoc-1(tm7125) V*, *isolate 1.7*
LW5521	*jjIs4688[pJKL1139.2(smoc-1p::4xnls::gfp::unc-54 3′UTR)+pRF4] I or IV*; *smoc-1(tm7125) V*, *isolate 2.5*
LW4878	*jjIs3900[pJKL1066.3(hlh-8p::nls::mCherry::lacZ)+ pCFJ90(myo-2p::mCherry)] IV*; *jjIs4694[pJKL1139.2(smoc-1p::4xnls::gfp::unc-54 3′UTR)+pRF4] V*, *isolate 1.2*
LW4879	*jjIs3900[pJKL1066.3(hlh-8p::nls::mCherry::lacZ)+ pCFJ90(myo-2p::mCherry)] IV*; *jjIs4694[pJKL1139.2(smoc-1p::4xnls::gfp::unc-54 3′UTR)+pRF4] V*, *isolate 2.4*
LW5656	*jjEx5656[pJKL1201(5kb smoc-1p::4xnls::gfp::unc-54 3′UTR)+pRF4]*
LW5657	*jjEx5657[pJKL1201(5kb smoc-1p::4xnls::gfp::unc-54 3′UTR)+pRF4]*
LW5658	*jjEx5658[pJKL1202(5kb smoc-1p::4xnls::gfp::2kb smoc-1 3′UTR)+pRF4]*
LW5659	*jjEx5658[pJKL1202(5kb smoc-1p::4xnls::gfp::2kb smoc-1 3′UTR)+pRF4]*
Strains with forced expression of *smoc-1* to assay for the Susm phenotype	
LW4812	*jjEx4812[pJKL1138.1(smoc-1p::smoc-1 cDNA::unc-54 3′UTR) + LiuFD188(myo-2p::mCherry)]*; *arIs37[secreted CC::gfp] I*; *ccIs4438[intrinsic CC::gfp] III*; *smoc-1(tm7125) V*; *sma-9(cc604) ayIs6[hlh-8p::gfp] X*
LW4813	*jjEx4813[pJKL1138.1(smoc-1p::smoc-1 cDNA::unc-54 3′UTR) + LiuFD188(myo-2p::mCherry)]*; *arIs37[secreted CC::gfp] I*; *ccIs4438[intrinsic CC::gfp] III*; *smoc-1(tm7125) V*; *sma-9(cc604) ayIs6[hlh-8p::gfp] X*
LW4810	*jjEx4810[pMSD4.4(smoc-1p::smoc-1 cDNA:: smoc-1 3′UTR) + LiuFD188(myo-2p::mCherry)]*; *arIs37[secreted CC::gfp] I*; *ccIs4438[intrinsic CC::gfp] III*; *smoc-1(tm7125) V*; *sma-9(cc604) ayIs6[hlh-8p::gfp] X*
LW4811	*jjEx4811[pMSD4.4(smoc-1p::smoc-1 cDNA:: smoc-1 3′UTR) + LiuFD188(myo-2p::mCherry)]*; *arIs37[secreted CC::gfp] I*; *ccIs4438[intrinsic CC::gfp] III*; *smoc-1(tm7125) V*; *sma-9(cc604) ayIs6[hlh-8p::gfp] X*
LW4619	*jjEx4619[pJKL1136.4(hlh-8p::smoc-1 mutant cDNA::unc-54 3′UTR)+ LiuFD61(mec-7p::rfp)]*; *arIs37[secreted CC::gfp] I*; *ccIs4438[intrinsic CC::gfp] III*; *smoc-1(tm7125) V*; *sma-9(cc604) ayIs6[hlh-8p::gfp] X*
LW4620	*jjEx4620[pJKL1136.4(hlh-8p::smoc-1 mutant cDNA::unc-54 3′UTR)+ LiuFD61(mec-7p::rfp)]*; *arIs37[secreted CC::gfp] I*; *ccIs4438[intrinsic CC::gfp] III*; *smoc-1(tm7125) V*; *sma-9(cc604) ayIs6[hlh-8p::gfp] X*
LW4687	*jjEx4687[pJKL1136.4(hlh-8p::smoc-1 cDNA::unc-54 3′UTR)+ LiuFD61(mec-7p::rfp)]*; *arIs37[secreted CC::gfp] I*; *ccIs4438[intrinsic CC::gfp] III*; *smoc-1(tm7125) V*; *sma-9(cc604) ayIs6[hlh-8p::gfp] X*
LW4650	*jjEx4650[pJKL1136.4(hlh-8p::smoc-1 cDNA::unc-54 3′UTR)+ LiuFD61(mec-7p::rfp)]*; *arIs37[secreted CC::gfp] I*; *ccIs4438[intrinsic CC::gfp] III*; *smoc-1(tm7125) V*; *sma-9(cc604) ayIs6[hlh-8p::gfp] X*
LW5147	*jjEx5147[pMSD18.4(ifb-2p::smoc-1 cDNA::unc-54 3′UTR)+ LiuFD188(myo-2p::mCherry)]*; *arIs37[secreted CC::gfp] I*; *ccIs4438[intrinsic CC::gfp] III*; *smoc-1(tm7125) V*; *sma-9(cc604) ayIs6[hlh-8p::gfp] X*
LW5148	*jjEx5148[pMSD18.4(ifb-2p::smoc-1 cDNA::unc-54 3′UTR) + LiuFD188(myo-2p::mCherry)]*; *arIs37[secreted CC::gfp] I*; *ccIs4438[intrinsic CC::gfp] III*; *smoc-1(tm7125) V*; *sma-9(cc604) ayIs6[hlh-8p::gfp] X*
LW5005	*jjEx5005[pMSD9.7(rab-3p::smoc-1 cDNA::unc-54 3′UTR) + LiuFD188(myo-2p::mCherry)]*; *arIs37[secreted CC::gfp] I*; *ccIs4438[intrinsic CC::gfp] III*; *smoc-1(tm7125) V*; *sma-9(cc604) ayIs6[hlh-8p::gfp] X*
LW5006	*jjEx5006[pMSD9.7(rab-3p::smo-c1 cDNA::unc-54 3′UTR) + LiuFD188(myo-2p::mCherry)]*; *arIs37[secreted CC::gfp] I*; *ccIs4438[intrinsic CC::gfp] III*; *smoc-1(tm7125) V*; *sma-9(cc604) ayIs6[hlh-8p::gfp] X*
LW5076	*jjEx5076[pMSD6.7(elt-3p::smoc-1 cDNA::unc-54 3′UTR) + LiuFD188(myo-2p::mCherry)]*; *arIs37[secreted CC::gfp] I*; *ccIs4438[intrinsic CC::gfp] III*; *smoc-1(tm7125) V*; *sma-9(cc604) ayIs6[hlh-8p::gfp] X*
LW5002	*jjEx5002[pMSD7.3(myo-2p::smoc-1 cDNA::unc-54 3′UTR) + LiuFD188(myo-2p::mCherry) + pBSIISK+]*; *arIs37[secreted CC::gfp] I*; *ccIs4438[intrinsic CC::gfp] III*; *smoc-1(tm7125) V*; *sma-9(cc604) ayIs6[hlh-8p::gfp] X*
LW5003	*jjEx5003[pMSD7.3(myo-2p::smoc-1 cDNA::unc-54 3′UTR) + LiuFD188(myo-2p::mCherry) + pBSIISK+]*; *arIs37[secreted CC::gfp] I*; *ccIs4438[intrinsic CC::gfp] III*; *smoc-1(tm7125) V*; *sma-9(cc604) ayIs6[hlh-8p::gfp] X*

(continued)

Table 1, *continued*

Strain identifier	Genotype
Strains with forced expression of *smoc-1* to assay for the body size phenotype	
LW5049	*jjEx5049[pJKL1137.2(hlh8p::smoc-1 cDNA::unc-54 3′UTR) + LiuFD188(myo-2p::mCherry)]; smoc-1(tm7125) V*
LW5050	*jjEx5050[pJKL1137.2(hlh8p::smoc-1 cDNA::unc-54 3′UTR) + LiuFD188(myo-2p::mCherry)]; smoc-1(tm7125) V*
LW5051	*jjEx5051[pMSD18.4(ifb-2p::smoc-1 cDNA::unc-54 3′UTR) + LiuFD188(myo-2p::mCherry)]; smoc-1(tm7125) V*
LW5052	*jjEx5052[pMSD18.4(ifb-2p::smoc-1 cDNA::unc-54 3′UTR) + LiuFD188(myo-2p::mCherry)]; smoc-1(tm7125) V*
LW5118	*jjEx5118[pMSD4.4(smoc-1p::smoc-1 cDNA::smoc-1 3′UTR) + LiuFD188(myo-2p::mCherry)]; smoc-1(tm7125) V*
LW4790	*jjEx4790[pMSD4.4(smoc-1p::smoc-1 cDNA::smoc-1 3′UTR) + LiuFD188(myo-2p::mCherry)]; smoc-1(tm7125)*
LW4791	*jjEx4791[pJKL1138.1(smoc-1p::smoc-1 cDNA::unc-54 3′UTR) + LiuFD188(myo-2p::mCherry)]; smoc-1(tm7125) V*
LW4850	*jjEx4850[pMSD7.3(myo-2p::smoc-1 cDNA::unc-54 3′UTR) + LiuFD188(myo-2p::mCherry) + pBSIIsk+]; smoc-1(tm7125) V*
LW4849	*jjEx4849[pMSD7.3(myo-2p::smoc-1 cDNA::unc-54 3′UTR) + LiuFD188(myo-2p::mCherry) + pBSIIsk+] smoc-1(tm7125) V*
LW5715	*jjEx4849[pMSD7.3(myo-2p::smoc-1 cDNA::unc-54 3′UTR) + LiuFD188(myo-2p::mCherry) + pBSIIsk+]; dbl-1(ok3749) V*
LW5716	*jjEx4849[pMSD7.3(myo-2p::smoc-1 cDNA::unc-54 3′UTR) + LiuFD188(myo-2p::mCherry) + pBSIIsk+]; dbl-1(ok3749) V*
LW4919	*jjEx4919[pMSD6.7(elt-3p::smoc-1 cDNA::unc-54 3′UTR) + LiuFD188(myo-2p::mCherry) + pBSIIsk+]; smoc-1(tm7125) V*
LW4853	*jjEx4853[pMSD6.7(elt-3p::smoc-1 cDNA::unc-54 3′UTR) + LiuFD188(myo-2p::mCherry) + pBSIIsk+]; smoc-1(tm7125) V*
LW4851	*jjEx4851[pMSD8.5(myo-3p::smoc-1 cDNA::unc-54 3′UTR) + LiuFD188(myo-2p::mCherry) + pBSIIsk+]; smoc-1(tm7125) V*
LW4852	*jjEx4852[pMSD8.5(myo-3p::smoc-1 cDNA::unc-54 3′UTR) + LiuFD188(myo-2p::mCherry) + pBSIIsk)]; smoc-1(tm7125) V*
LW4906	*jjEx4906[pMSD9.7(rab-3p::smoc-1 cDNA::unc-54 3′UTR) + LiuFD188(myo-2p::mCherry)]; smoc-1(tm7125) V*
Strains expressing the human *SMOC* genes	
LW4918	*jjEx4918[pMSD9.7(rab-3p::smoc-1 cDNA::unc-54 3′UTR) + LiuFD188(myo-2p::mCherry)]; smoc-1(tm7125) V*
LW5664	*jjEx5664[pJKL1178(Celsmoc-1p::hsmoc1 ORF::unc-54 3′UTR) + pJKL724.1(myo-3p::RFP)]; smoc-1(tm7125) V*
LW5666	*jjEx5666[pJKL1178(Celsmoc-1p::hsmoc1 ORF::unc-54 3′UTR) + pJKL724.1(myo-3p::RFP)]; smoc-1(tm7125) V*
LW5668	*jjEx5668[pJKL1179(Celsmoc-1p::hsmoc2 ORF::unc-54 3′UTR) + pJKL724.1(myo-3p::RFP)]; smoc-1(tm7125) V*
LW5670	*jjEx5670[pJKL1179(Celsmoc-1p::hsmoc2 ORF::unc-54 3′UTR) + pJKL724.1(myo-3p::RFP)]; smoc-1(tm7125) V*
LW5077	*jjEx5077[pJKL1150(Celsmoc-1p::hsmoc1 ORF::Celsmoc-1 3′UTR) + LiuFD188(myo-2p::mCherry)]; arIs37[secreted CC::gfp] I; ccIs4438[intrinsic CC::gfp] III; smoc-1(tm7125) V; sma-9(cc604) ayIs6[hlh-8p::gfp] X*
LW5078	*jjEx5078[pJKL1150(Celsmoc-1p::hsmoc1 ORF::Celsmoc-1 3′UTR) + LiuFD188(myo-2p::mCherry)]; arIs37[secreted CC::gfp] I; ccIs4438[intrinsic CC::gfp] III; smoc-1(tm7125) V; sma-9(cc604) ayIs6[hlh-8p::gfp] X*
LW5079	*jjEx5079[pJKL1151(Celsmoc-1p::hsmoc2 ORF::Celsmoc-1 3′UTR) + LiuFD188(myo-2p::mCherry)]; arIs37[secreted CC::gfp] I; ccIs4438[intrinsic CC::gfp] III; smoc-1(tm7125) V; sma-9(cc604) ayIs6[hlh-8p::gfp] X*
LW5080	*jjEx5080[pJKL1151(Celsmoc-1p::hsmoc2 ORF::Celsmoc-1 3′UTR) + LiuFD188(myo-2p::mCherry)]; arIs37[secreted CC::gfp] I; ccIs4438[intrinsic CC::gfp] III; smoc-1(tm7125) V; sma-9(cc604) ayIs6[hlh-8p::gfp] X*
LW5455	*jjEx5455[pJKL1178(Celsmoc-1p::hsmoc1 ORF::unc-54 3′UTR) + pJKL724.1(myo-3p::RFP)]; arIs37[secreted CC::gfp] I; ccIs4438[intrinsic CC::gfp] III; smoc-1(tm7125) V; sma-9(cc604) ayIs6[hlh-8p::gfp] X*
LW5456	*jjEx5456[pJKL1178(Celsmoc-1p::hsmoc1 ORF::unc-54 3′UTR) pJKL724.1(myo-3p::RFP)]; arIs37[secreted CC::gfp] I; ccIs4438[intrinsic CC::gfp] III; smoc-1(tm7125) V; sma-9(cc604) ayIs6[hlh-8p::gfp] X*
LW5457	*jjEx5457[pJKL1179(Celsmoc-1p::hsmoc2 ORF::unc-54 3′UTR) + pJKL724.1(myo-3p::RFP)]; arIs37[secreted CC::gfp] I; ccIs4438[intrinsic CC::gfp] III; smoc-1(tm7125) V; sma-9(cc604) ayIs6[hlh-8p::gfp] X*
LW5458	*jjEx5458[pJKL1179(Celsmoc-1p::hsmoc2 ORF::unc-54 3′UTR) + pJKL724.1(myo-3p::RFP)]; arIs37[secreted CC::gfp] I; ccIs4438[intrinsic CC::gfp] III; smoc-1(tm7125) V; sma-9(cc604) ayIs6[hlh-8p::gfp] X*

Susm, suppression of *sma-9(0)* M-lineage defect.

using the iVision software (Biovision Technology). Subsequent image analysis was performed using Fiji (Schindelin *et al.* 2012). The RAD-SMAD reporter assay was carried out as previously described (Tian *et al.* 2013).

Body size measurements

Body size measurement assays were conducted as previously described (Tian *et al.* 2013). Hermaphrodite animals at the gravid adult stage were collected and treated with hypochlorite. The resulting embryos were allowed to hatch in M9 buffer at 16°. Synchronized L1s were plated onto NGM plates and allowed to grow at 20°. Worms were washed off the plates, treated with 0.3% sodium azide, and mounted onto 2% agarose pads. Hermaphrodite worms were imaged at the L4.3 stage based on vulval development (Mok *et al.* 2015). Images were taken by a Hamamatsu Orca-ER camera using the iVision software (Biovision Technology). Body sizes were measured from images using the segmented line tool of Fiji. An ANOVA and Tukey's honest significant difference (HSD) were conducted to test for differences in body size between genotypes using R (R Core Team 2015).

Suppression of sma-9(0) M-lineage defect assay

For the suppression of *sma-9(0)* M-lineage defect (Susm) assay, worms were grown at 20°, and then the number of animals with four CCs and six CCs were tallied across three to seven plates for each genotype. For the Susm rescue experiments shown in Figure 7B and Figure 8B, we used R to generate a general linear model with binomial error and a logit link function designating transgenic state as the explanatory function. The Wald statistic was used to determine if transgenic state (transgenic *vs.* nontransgenic worms within the same line) is associated with CC number.

Dauer formation assay

Dauer formation assay was conducted under nondauer-inducing conditions as previously described (Vowels and Thomas 1992). Ten adult hermaphrodites were placed on a

Table 2 Plasmid constructs generated in this study

Plasmid name	Construct information	
Translational and transcriptional reporter constructs		
pJKL1128	*2 kb smoc-1p::smoc-1 genomic::2 kb smoc-1 3′UTR*	
pMSD4	*2 kb smoc-1p::smoc-1 cDNA::2 kb smoc-1 3′UTR*	
pJKL1138	*2 kb smoc-1p::smoc-1 cDNA::unc-54 3′UTR*	
pJKL1139	*2 kb smoc-1p::4xnls::gfp::unc-54 3′UTR*	
pJKL1201	*5 kb smoc-1p::4xnls::gfp::unc-54 3′UTR*	
pJKL1202	*5 kb smoc-1p::4xnls::gfp::2 kb smoc-1 3′UTR*	
Tissue specific expression constructs		
pJKL1137	*hlh-8p::smoc-1 cDNA::unc-54 3′UTR*	M lineage
pJKL1136	*hlh-8p::smoc-1 cDNA-S103P::unc-54 3′UTR*	M lineage
pMSD6	*elt-3p::smoc-1 cDNA::unc-54 3′UTR*	hypodermis
pMSD7	*myo-2p::smoc-1 cDNA::unc-54 3′UTR*	pharyngeal muscles
pMSD8	*myo-3p::smoc-1 cDNA::unc-54 3′UTR*	body wall muscles
pMSD9	*rab-3p::smoc-1 cDNA::unc-54 3′UTR*	pan neurons
pMSD18	*ifb-2p::smoc-1 cDNA::unc-54 3′UTR*	intestine
pJKL1217	*dpy-30p::smoc-1 cDNA::unc-54 3′UTR*	ubiquitous
Constructs to express human *SMOC* genes		
pJKL1150	*2 kb smoc-1p::huSMOC1 ORF::smoc-1 3′UTR*	
pJKL1151	*2 kb smoc-1p::huSMOC2 ORF::smoc-1 3′UTR*	
pJKL1178	*2 kb smoc-1p::CelSP::huSMOC1 chimera::unc-54 3′UTR*	
pJKL1179	*2 kb smoc-1p::CelSP::huSMOC2 chimera::unc-54 3′UTR*	

6-cm NGM plate (five plates per strain at each temperature) and allowed to lay eggs for < 8 hr. Adults were removed and plates were placed at the test temperature. When nondauer worms became young adults, the numbers of dauer and nondauer worms on each plate were scored. Using R, we tested for differences in dauer formation between genotypes using an ANOVA followed by Tukey's HSD.

Data availability

Strains and plasmids are available upon request. The authors affirm that all data necessary for confirming the conclusions of the article are present within the article, figures, and tables.

Results

Mutations in T04F3.2 suppress the mesoderm defects of sma-9(0) mutants

In a previous *sma-9* suppressor screen, we uncovered a novel complementation group named *susm-1* that includes three alleles, *jj65*, *jj85*, and *jj180* (Liu *et al.* 2015) (Table 3), which suppressed the *sma-9(0)* M-lineage defect at high penetrance. Whole-genome sequencing (WGS) of the three alleles using the SNP-WGS method described in Liu *et al.* (2015) identified molecular lesions in the uncharacterized gene T04F3.2: *jj65* and *jj85* are missense mutations C210Y and E105K, respectively, while *jj180* is a nonsense mutation denoted Q180Stop (Figure 2, A and B). To confirm that T04F3.2 is the corresponding gene for this complementation group, we obtained two deletion alleles that delete most of the coding region of T04F3.2, *tm7000*, and *tm7125* (Figure 2A), and found that both alleles suppressed the *sma-9(0)* M-lineage defect to near 100% (Figure 1C and Table 3). Pairwise complementation tests between *tm7000* and *jj65*, *jj85*, or *jj180*, showed that *tm7000* failed to complement all three alleles in their suppression of the *sma-9(0)* M-lineage defect (Table 3). Subsequent *sma-9(0)* suppressor screens conducted in the laboratory identified three additional alleles of this complementation group: *jj109*, *jj115*, and *jj139*. WGS followed by Sanger sequencing showed that all three alleles contain nonsense mutations in T04F3.2: W13Stop for both *jj115* and *jj139*, and W176Stop for *jj109* (Figure 2, A and B). Finally, a transgene containing the T04F3.2 genomic region including 2-kb upstream sequences, the entire coding region with introns, and 2-kb downstream sequences rescued the *sma-9(0)* suppression phenotype of *tm7125* mutants (Table 3). Collectively, these results demonstrated that T04F3.2 is the corresponding gene for the *susm-1* locus. The nature of the molecular lesions in *tm7000*, *tm7125*, *jj109*, *jj115*, *jj139*, and *jj180*, the near 100% penetrance of their Susm phenotypes, and their similar body size phenotypes (see below), suggest that all of these alleles are putative null alleles. For ease of genotyping, most of our subsequent analysis was carried out using the *tm7125* allele.

T04F3.2 encodes a predicted SMOC protein: SMOC-1

T04F3.2 is predicted to encode a protein of 260 amino acids. It contains a predicted signal peptide, a TY domain, and a secreted protein acidic and rich in cysteine (SPARC) EC-binding region (Figure 2). The EC domain is predicted to contain a pair of helix-loop-helix EF hand calcium-binding motifs (Hohenester *et al.* 1996; Vannahme *et al.* 2002). The predicted T04F3.2 protein is most similar to the human secreted modular calcium-binding proteins SMOC1 and SMOC2 (Vannahme *et al.* 2002, 2003), and the *D. melanogaster* SMOC homolog Pentagone/Magu (Vuilleumier *et al.* 2010). A Basic Local Alignment Search Tool search against the *C. elegans* genome showed that T04F3.2 is the

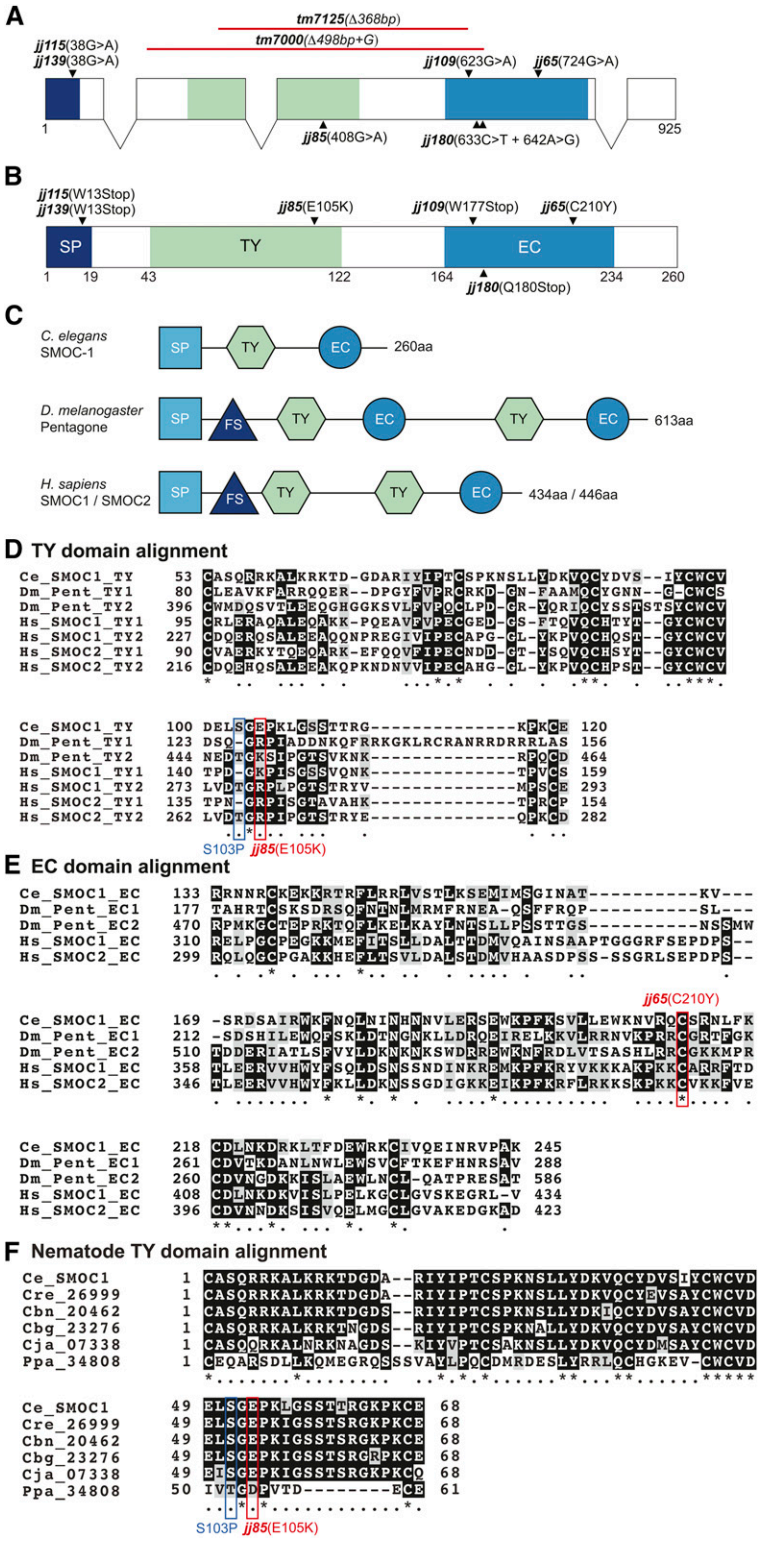

Figure 2 SMOC-1 is conserved from *C. elegans* to human. (A and B) Schematics of the *C. elegans smoc-1* gene (A) and the predicted SMOC-1 protein (B), respectively, showing the domain structure and the molecular lesions of various mutant alleles. (C) Schematic representation of *C. elegans* SMOC-1, *D. melanogaster* Pentagone, and *H. sapiens* SMOC1 and SMOC2, showing their domain structures. The two human SMOC proteins are of different lengths but share similar domain structures. (D and E) Alignment of the TY (D) and EC (E) domains from *C. elegans* SMOC-1, *D. melanogaster* Pentagone, and *H. sapiens* SMOC1 and SMOC2. Multiple copies of a certain domain in the same protein are numbered in order from the N- to the C-termini. (F) Alignment of the TY domains from SMOC-1 homologs in various nematode species. In (D–F), identical or conserved amino acids are shown on a black or gray background, respectively. Red boxes highlight residues mutated in certain *smoc-1* alleles. Blue box indicates the residue changed in a *smoc-1* cDNA clone that rendered the protein nonfunctional. Cbg, *C. briggsae*; Cbn, *C. brenneri*; Ce, *C. elegans*; Cel, *C. elegans*; Cja, *C. japonica*; Cre, *C. remanei*; Dm, *D. melanogaster*; EC, secreted protein acidic and rich in cysteine (SPARC) extracellular calcium-binding domain; FS, follistatin-like domain; Hs, *H. sapiens*; Ppa, *Pristionchus pacificus*; SP, signal peptide; TY, thyroglobulin type I-like repeat.

only SMOC homolog. Therefore, we have named this gene *smoc-1* and its corresponding protein SMOC-1.

SMOC proteins are matricellular proteins that are in the same family as SPARC/BM-40/osteonectin (Bradshaw 2012). The domain arrangement of SMOC proteins varies across species. The *C. elegans* SMOC-1 protein is predicted to have one TY domain, one EC domain, and completely lack the follistatin domain that is present in other SMOC proteins (Figure 2C). Within the TY domain, SMOC-1 shares ~30% amino acid identity and 50% similarity with human SMOC1 and SMOC2, and contains a CWCV tetrapeptide sequence and an additional four conserved cysteines that are characteristic

Table 3 Mutations in *smoc-1* suppress the *sma-9(0)* M-lineage defects

Genotype	Susm penetrance[a] (# of animals examined)
sma-9(cc604)	–
smoc-1(jj65); sma-9(cc604)	84% (*N* = 255)[b]
smoc-1(jj85); sma-9(cc604)	78% (*N* = 240)[b]
smoc-1(jj180); sma-4(jj70); sma-9(cc604)	98% (*N* = 80)[b,c]
smoc-1(jj180); sma-9(cc604)	98% (*N* = 319)[c]
sma-4(jj70); sma-9(cc604)	0% (*N* > 100)[c]
sma-4(e729); sma-9(cc604)	100% (*N* = 61)[d]
smoc-1(tm7000); sma-9(cc604)	97% (*N* = 134)
smoc-1(tm7125); sma-9(cc604)	98% (*N* = 686)
smoc-1(tm7000)/jj65 or +/jj65; sma-9(cc604)	67% (*N* = 51)[e]
smoc-1(tm7000)/jj85 or +/jj85; sma-9(cc604)	46% (*N* = 24)[e]
smoc-1(tm7000)/jj180 or +/jj180; sma-9(cc604)	58% (*N* = 26)[e]
smoc-1(jj109); sma-9(cc604)	99% (*N* = 107)
smoc-1(jj115); sma-9(cc604)	100% (*N* = 95)
smoc-1(jj139); sma-9(cc604)	100% (*N* = 128)
smoc-1(tm7125); sma-9(cc604); jjEx4490[smoc-1p::smoc-1 genomic::smoc-1 3′UTR], line 1	32% (*N* = 111)
smoc-1(tm7125); sma-9(cc604); jjEx4491[smoc-1p::smoc-1 genomic::smoc-1 3′UTR], line 2	26% (*N* = 101)
smoc-1(tm7125); sma-9(cc604); jjEx4810[smoc-1p::smoc-1 cDNA::smoc-1 3′UTR], line 1	2% (*N* = 278)
smoc-1(tm7125); sma-9(cc604); jjEx4811[smoc-1p::smoc-1 cDNA::smoc-1 3′UTR], line 2	1% (*N* = 498)
smoc-1(tm7125); sma-9(cc604); jjEx4812[smoc-1p::smoc-1 cDNA::unc-54 3′UTR], line 1	17% (*N* = 481)
smoc-1(tm7125); sma-9(cc604); jjEx4813[smoc-1p::smoc-1 cDNA::unc-54 3′UTR], line 2	23% (*N* = 792)
smoc-1(tm7125); sma-9(cc604); jjEx4650[hlh-8p::smoc-1 cDNA::unc-54 3′UTR], line 1	15% (*N* = 186)
smoc-1(tm7125); sma-9(cc604); jjEx4612[hlh-8p::smoc-1 cDNA::unc-54 3′UTR], line 3	17% (*N* = 214)
smoc-1(tm7125); sma-9(cc604); jjEx4620[hlh-8p::smoc-1 cDNA-S103P::unc-54 3′UTR], line 1	86% (*N* = 95)
smoc-1(tm7125); sma-9(cc604); jjEx4674[hlh-8p::smoc-1 cDNA-S103P::unc-54 3′UTR], line 2	92% (*N* = 100)

CC, coelomocyte; Susm, suppression of *sma-9(0)* M-lineage defect.

[a] The Susm penetrance refers to the percent of animals with one or two M-derived CCs as scored by the *CC::GFP* reporter.

[b] Data taken from Liu *et al.* (2015).

[c] The *jj70* strain described in our previous publication (Liu *et al.* 2015) carries a mutation in *sma-4*(S110L), as well as a mutation in *smoc-1* (Q180Stop). To avoid confusion, we have designated the *sma-4* mutation as *jj70*, and the mutation in *smoc-1* as *jj180*. As shown here, *sma-4(jj70)* failed to suppress *sma-9(0)*, while *smoc-1(jj180)* suppressed *sma-9(0)*.

[d] Data taken from Foehr *et al.* (2006).

[e] Complementation tests were performed by crossing *tm7000/+*; *cc604* males with *jj65 (jj85 or jj180)*; *cc604* hermaphrodites and scoring the cross progeny for the number of CCs. All progeny would have four CCs if the tested alleles complemented each other, while ∼50% of the progeny would have six CCs if the tested alleles failed to complement each other. The partial dominance of each of the *jj* alleles tested (Liu *et al.* 2015) may have contributed to the observed percentage being slightly above 50%.

of the TY domain (Figure 2D). The EC domain of SMOC-1 shares ∼25% amino acid identity and 45% similarity with those of the human SMOC proteins. Among the conserved residues in the EC domain are four cysteines thought to be involved in disulfide-bond formation (Busch *et al.* 2000).

The locations of the molecular lesions in our *smoc-1* mutant alleles suggest that both the TY and EC domains are important for SMOC-1 function. *jj85* is a mutation in the TY domain, changing amino acid 105 from a glutamic acid to a lysine (E105K, Figure 2, B and D). Although the change appears to make this residue more similar to its counterpart (arginine or lysine) in the fly and human SMOC proteins (Figure 2D), we noted that E105 is conserved in multiple nematode species (Figure 2F). We also obtained a *smoc-1* cDNA clone that has a single-base mutation changing amino acid 103 from a conserved serine to proline (Figure 2D). This mutant *smoc-1* cDNA (S103P) failed to rescue the *smoc-1(0)* Susm phenotype, while the wild-type (WT) *smoc-1* cDNA under the same regulatory elements successfully rescued the *smoc-1(0)* Susm phenotype (Table 3), again highlighting the importance of the TY domain for SMOC-1 function. Similarly, the EC domain is also critical for SMOC-1 function, because a change of the conserved cysteine residue at amino acid 210 to tyrosine (C210Y) in *jj65* significantly compromised the function of SMOC-1 (Figure 2, B and E and Table 3).

SMOC-1 functions within the BMP pathway to positively regulate BMP signaling

We have previously shown that mutations in BMP pathway components specifically suppress the *sma-9(0)* M-lineage defect (Foehr *et al.* 2006; Liu *et al.* 2015). The highly penetrant Susm phenotype of multiple *smoc-1* alleles suggests that SMOC-1 may function in the BMP pathway. BMP pathway mutants are known to exhibit altered body sizes (Savage-Dunn and Padgett 2017). We measured the body sizes of *smoc-1* single-mutant animals and found that they all have a reproducibly smaller body size (∼95%) compared to WT animals at the same developmental stage (Figure 3, A, B, and D). This smaller body size can be rescued by a WT *smoc-1* transgene (Figure 3D). Moreover, transgenic *smoc-1* mutant animals carrying this transgene are significantly longer than WT animals (Figure 3D). The increased body size is likely

caused by the presence of multiple gene copies within the transgene generated using standard *C. elegans* transgenic approaches, which often results in overexpression of the gene (Mello *et al.* 1991). We have subsequently integrated the *smoc-1* transgene in the WT background (*jjIs5119*, Table 1). Again, *jjIs5119* [which we have referred to as *smoc-1(OE)*] animals are significantly longer than WT animals (Figure 4B). Thus, *smoc-1* appears to function in a dose-dependent manner to positively regulate body size.

To determine whether *smoc-1* functions within the BMP pathway to regulate body size, we generated double mutants between *smoc-1(tm7125)* and null mutations in various BMP pathway components, and measured their body lengths. As shown in Figure 4A, *dbl-1(ok3749) smoc-1(tm7125)* double mutants were as small as *dbl-1(ok3749)* single mutants. Similarly, *sma-3(jj3)*; *smoc-1(tm7125)* and *sma-6(jj1)*; *smoc-1(tm7125)* double mutants were as small as *sma-3(jj3)* and *sma-6(jj1)* single mutants, respectively. These observations indicate that *smoc-1* functions within the BMP pathway, rather than in a parallel pathway, to regulate body size.

In addition to body size, BMP pathway mutants also exhibit male tail defects and the mutant males cannot mate (Savage *et al.* 1996; Krishna *et al.* 1999; Suzuki *et al.* 1999). We generated *smoc-1(tm7125)* males and found that they mated well with WT hermaphrodites to produce cross progeny, suggesting that *smoc-1(tm7125)* males do not have severe male tail-patterning defects. This is not surprising as previous studies have demonstrated that male tail development is not affected when there is a partial reduction of BMP signaling (Krishna *et al.* 1999).

We also examined the expression of the RAD-SMAD reporter, which we have previously shown serves as a direct readout of BMP signaling (Tian *et al.* 2010). While *smoc-1(tm7125)* mutants did not exhibit significant changes in the expression of the RAD-SMAD reporter (data now shown), the *smoc-1(OE)* lines showed a significant increase in the level of RAD-SMAD reporter expression (Figure 4, G and H). We reasoned that the change of RAD-SMAD reporter expression in *smoc-1(tm7125)* mutants may be too small to detect, given that *smoc-1(tm7125)* mutants only exhibit a ~5% reduction in body size compared to WT animals (see above). Nevertheless, our findings are consistent with SMOC-1 acting in the BMP pathway to positively promote BMP signaling.

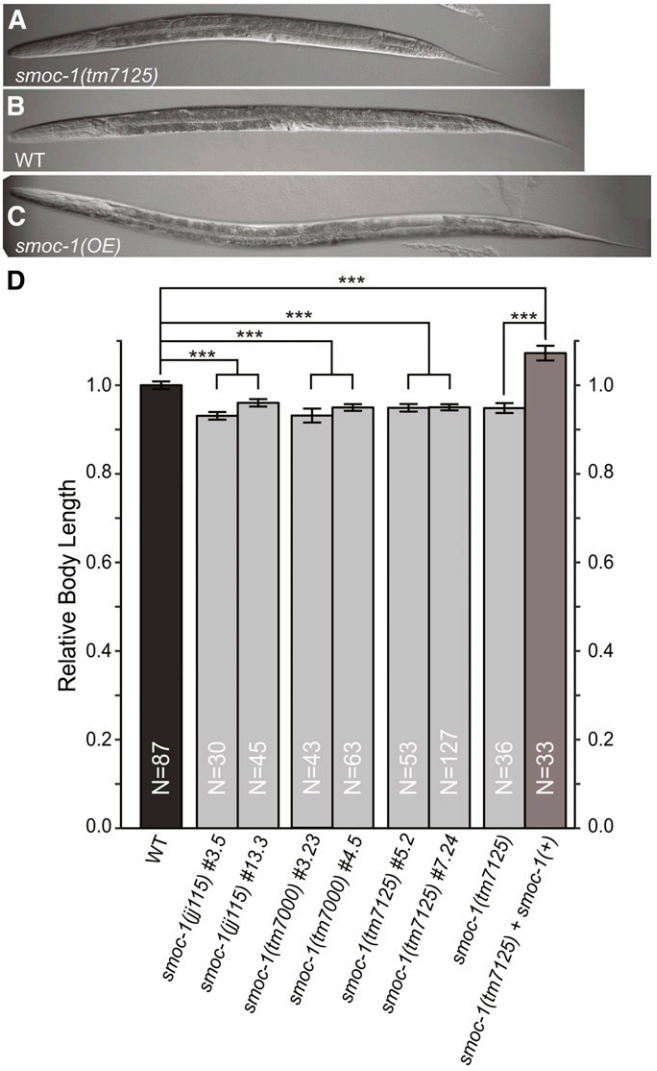

Figure 3 SMOC-1 regulates body size. (A–C) DIC images showing *smoc-1(tm7125)* (A), WT (B), and *smoc-1(OE)* (C) worms at the larval L4.3 stage. (D) Relative body length of developmental stage-matched WT and various *smoc-1* mutant worms. Each *smoc-1* mutant allele was outcrossed with N2 for at least three times, and two independent isolates for each allele (#s following the allele name) were used for body size measurement. The *smoc-1(+)* transgene was pMSD4*[2 kb smoc-1p::smoc-1 cDNA::2 kb smoc-1 3′UTR]*. The body length of WT worms was set to 1.0. Error bars represent 95% C.I. An ANOVA followed by Tukey's honest significant difference was used to test for differences between genotypes. *** $P <$ 0.0001. WT, wild-type.

SMOC-1 functions through the BMP ligand to promote BMP signaling in regulating body size

The long body size phenotype caused by *smoc-1* overexpression provided us with a useful tool to determine where in the BMP signaling pathway SMOC-1 functions. We conducted genetic epistasis analysis by generating double mutants between *smoc-1(OE)* and null mutations in core components of the BMP pathway that are known to cause a small body size. As shown in Figure 4B, *smoc-1(OE)*; *dbl-1(ok3749)* double mutants and *smoc-1(OE)*; *sma-3(tm4625)* double mutants are as small as *dbl-1(ok3749)* and *sma-3(tm4625)* single mutants, respectively. These results provide further support for the conclusion that SMOC-1 functions within the BMP pathway to regulate body size. More importantly, our genetic epistasis results demonstrate that SMOC-1 functions upstream of the BMP ligand DBL-1 in the same genetic pathway to regulate body size, and that the function of SMOC-1 as a positive modulator of body size is dependent on DBL-1.

SMOC-1 and LON-2/glypican function antagonistically to modulate BMP signaling in regulating body size

Previous studies have shown that the glypican LON-2 functions genetically upstream of DBL-1/BMP and acts as a

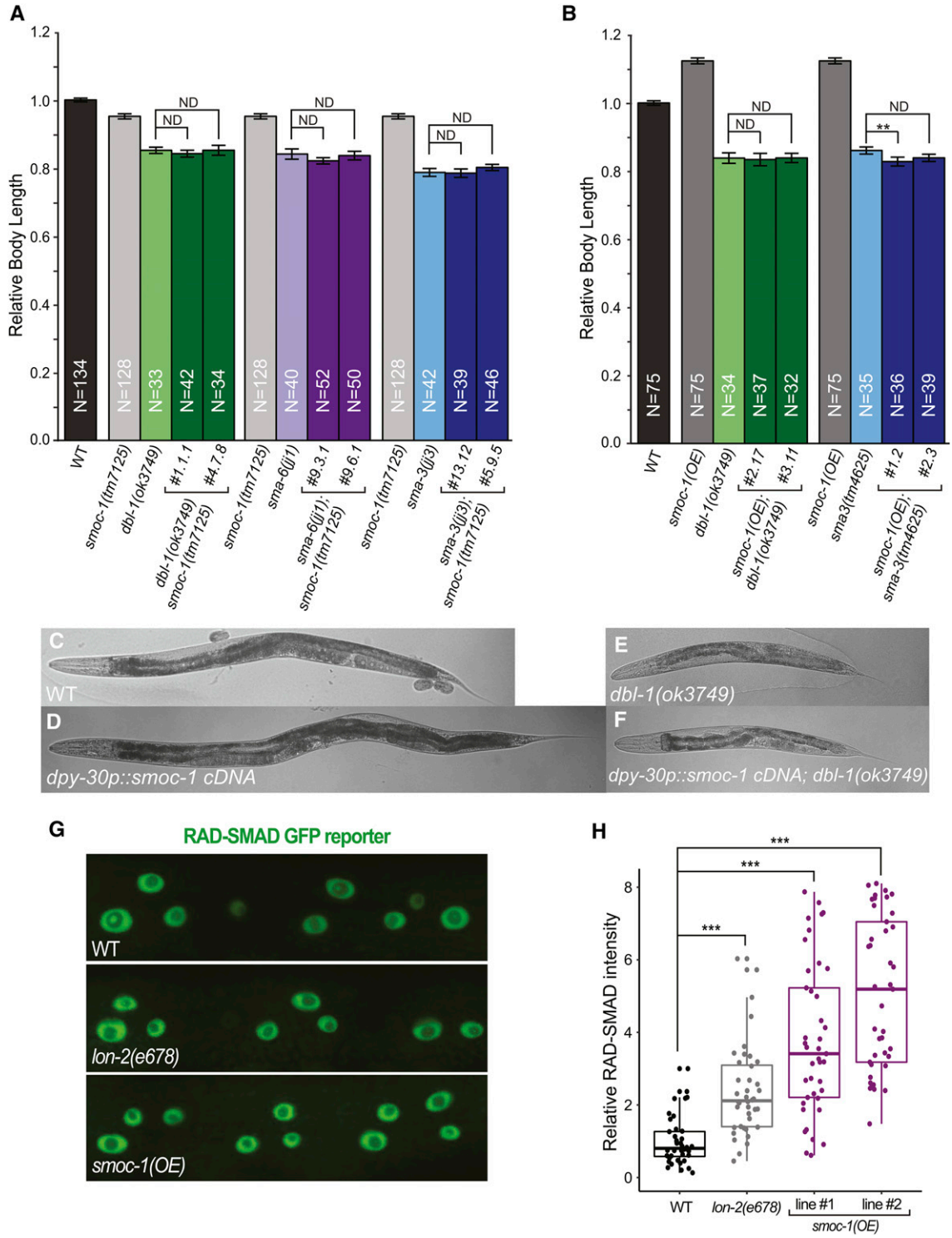

Figure 4 SMOC-1 functions through the BMP ligand to positively regulate BMP signaling. (A and B) Relative body length of developmental stage-matched WT and various mutant worms, including double mutants between *smoc-1(tm7125)* and null mutants in the BMP pathway (A), and double mutants between *smoc-1(OE)* and null mutants in the BMP pathway (B). Two independent isolates for each double-mutant combination were used for body size measurement. The body length of WT worms was set to 1.0. Error bars represent 95% C.I. (C–F) Representative images showing the body size of a WT worm (C), a WT worm carrying a *[dpy-30p*::*smoc-1 cDNA*::*unc-54 3′UTR]* transgene (D), a *dbl-1(ok3749)* worm (E), and a *dbl-1(ok3749)* worm carrying the *[dpy-30p*::*smoc-1 cDNA*::*unc-54 3′UTR]* transgene (F). (G) Representative GFP images showing RAD-SMAD reporter expression in hypodermal nuclei of WT, *lon-2(e678)*, and *smoc-1(OE)* worms, respectively. (H) Boxplot showing the relative RAD-SMAD GFP fluorescence intensity in WT (set to 1.0), *lon-2(e678)*, and two independent isolates of *smoc-1(OE)* worms. Each data point represents an average of the GFP fluorescence intensity from five hypodermal nuclei in one worm. Approximately 40 worms were examined per genotype. For (A, B, and D), an ANOVA followed by Tukey's honest significant difference was used to test for differences between genotypes. *** $P < 0.0001$. ND, no difference; WT, wild-type.

negative regulator of BMP signaling (Gumienny *et al.* 2007). We performed double-mutant analysis, and dissected the relationship between SMOC-1 and LON-2/glypican. We first measured the body length of double-null mutants between *smoc*-1 and *lon-2*. As shown in Figure 5A, *smoc-1(tm7125)*; *lon-2(e678)* double-null mutants exhibited an intermediate body size compared to either single-null mutant. In particular, the body size of *smoc-1(tm7125)*; *lon-2(e678)* double mutants is similar to WT animals. These observations suggest that SMOC-1 and LON-2/glypican antagonize each other in regulating body size. Interestingly, *smoc-1(OE)*; *lon-2(e678)* worms are longer than either *smoc-1(OE)* animals or *lon-2(e678)* single mutants (Figure 5B). Thus, overexpressing *smoc-1* is capable of further increasing the body size of worms that completely lack LON-2/glypican. Taken together, our genetic analysis between *lon-2* and *smoc-1* suggests that SMOC-1 and LON-2/glypican function independently and antagonistically to modulate BMP signaling in regulating body size.

SMOC-1 does not play a major role in the TGFβ-like dauer pathway

In addition to the BMP pathway, *C. elegans* has a TGFβ-like signaling pathway that regulates dauer development (Savage-Dunn and Padgett 2017). To determine if SMOC-1 plays a role in the TGFβ-like dauer pathway, we first assayed dauer formation of worms with different levels of *smoc-1* expression. *smoc-1(tm7125)* and *smoc-1(OE)* single-mutant worms did not exhibit any constitutive or defective dauer formation phenotype at any of the temperatures tested (Table 4, data not shown), suggesting that SMOC-1 does not play a major role in the TGFβ-like dauer pathway. Next, we generated double-mutant worms carrying both *smoc-1(tm7125)* and mutations in the TGFβ ligand DAF-7/TGFβ or the type 1 receptor DAF-1/RI (Georgi *et al.* 1990; Ren *et al.* 1996), and examined them for the constitutive dauer formation (Daf-c) phenotype (Table 1). While *smoc-1(tm7125)* partially suppressed the Daf-c phenotype of *daf-7(e1372)* at 20°, a similar trend was not observed at either 15 or at 25°. Similarly, *smoc-1(tm7125)* did not exhibit any consistent suppression or enhancement of the Daf-c phenotype of two *daf-1* mutant alleles (Table 4). These results suggest that SMOC-1 does not play a major role in the TGFβ-like dauer pathway, although we cannot rule out a minor buffering function of SMOC-1 in this pathway.

Because of the genetic interaction that we observed between *smoc-1* and *lon-2*, we also tested whether LON-2/glypican plays a role in the TGFβ-like dauer pathway by performing similar double-mutant analysis as described for *smoc-1*. At 20°, *lon-2(e678)* showed partial suppression of the Daf-c phenotype of *daf-7(e1372)* (Table 5), but a similar trend was not observed at 15 or at 25° (Table 5). As seen with *smoc-1(tm7125)*, *lon-2(e678)* also did not consistently enhance or suppress the Daf-c phenotype of a TGFβ receptor mutation, *daf-1(m213)*. Thus, like SMOC-1, LON-2 does not appear to play a major role, but may play a minor modulatory role, in the TGFβ dauer pathway.

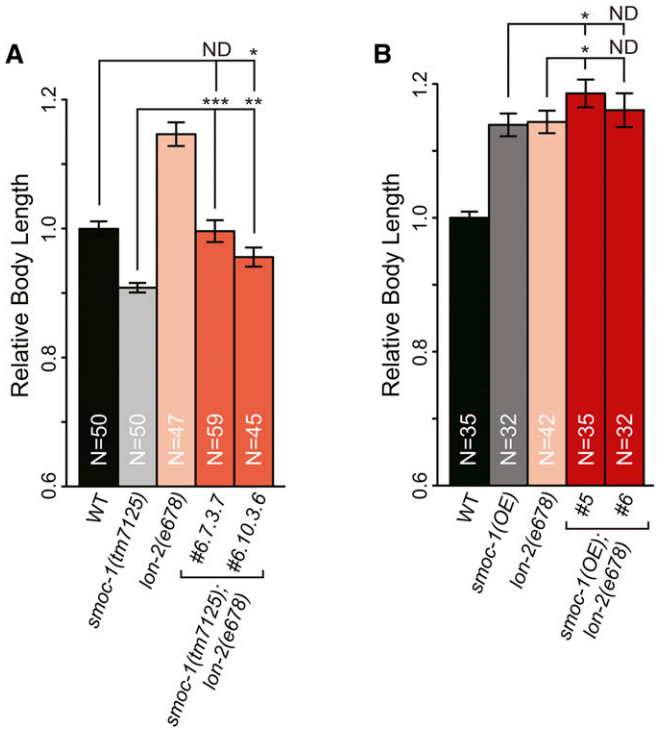

Figure 5 SMOC-1 antagonizes LON-2/glypican in regulating body size. Relative body length of developmental stage-matched WT (set to 1.0) and various mutant worms, including double mutants between *smoc-1(tm7125)* null and *lon-2(e678)* null (A), and double mutants between *smoc-1(OE)* and *lon-2(e678)* null (B). The body size of *smoc-1(tm7125)*; *lon-2(e678)* double-null mutants is similar to that of WT animals, while *smoc-1(OE)*; *lon-2(e678)* double mutants are longer than either one. Error bars represent 95% C.I. An ANOVA followed by Tukey's honest significant difference was used to test for differences between genotypes. * $P <$ 0.01, ** $P < 0.001$, and *** $P < 0.0001$. ND, no difference; WT, wild-type.

smoc-1 is expressed in the pharynx, intestine, and posterior hypodermis

Since *smoc-1* is predicted to encode a secreted protein, we first attempted to identify the cells that express *smoc-1*. As described above, a *smoc-1* genomic fragment containing 2-kb upstream sequences, the entire coding region with introns, and 2-kb downstream sequences (pJKL1128, Table 2) can rescue the Susm and body size phenotypes of *smoc-1(tm7125)* mutants (Figure 6A and Table 3). The same promoter element driving the *smoc-1* cDNA with its own 3′-UTR or with the *unc-54* 3′-UTR rescued both the small body size and the Susm phenotypes of *smoc-1(tm7125)* mutants (Figure 6A and Table 3), suggesting that the regulatory elements required for SMOC-1 function in BMP signaling reside in the 2-kb upstream sequences. Therefore, we generated a transcriptional reporter *pJKL1139[smoc-1 2 kb promoter::4xnls::gfp::unc-54 3′UTR]* (Table 2). We also generated two additional transcriptional reporters using 5-kb *smoc-1* upstream sequences (*pJKL1201[smoc-1 5kb promoter::4xnls::gfp::unc-54 3′UTR]* and *pJKL1202[smoc-1 5kb promoter::4xnls::gfp::2 kb smoc-1 3′UTR]*, Table 2). All three reporters showed similar expression patterns in transgenic animals. Therefore, we focused on

Table 4 SMOC-1 does not play a significant role in the TGFβ dauer pathway

Genotype	15°C % Daf-c (*n*)	20°C % Daf-c (*n*)	25°C % Daf-c (*n*)
smoc-1(tm7125)	0 (858)	0 (828)	0 (863)
jjIs5119[smoc-1(OE)]	0 (541)	0 (792)	0 (574)
daf-7(e1372)	30.2 ± 4.5 (348)	92.8 ± 2.9 (794)	99.8 ± 0.3 (954)
daf-7(e1372); smoc-1(tm7125) #1	33.8 ± 14.8 (142)	82.5 ± 9.3 (748)[a]	99.6 ± 0.3 (1102)
daf-7(e1372); smoc-1(tm7125) #2	26.4 ± 7.7 (148)	72.0 ± 8.3 (343)[a]	100 (1115)
daf-1(m40)	0 (485)	44.9 ± 7.4 (1059)	100 (964)
daf-1(m40); smoc-1(tm7125) #1	0 (589)	57.2 ± 16.4 (1567)[a]	99.9 ± 0.2 (970)
daf-1(m40); smoc-1(tm7125) #2	0 (483)	24.0 ± 8.8 (721)[a]	100 (518)
daf-1(m213)	0 (469)	99.4 ± 0.6 (867)	100 (1174)
daf-1(m213); smoc-1(tm7125) #1	0 (603)	98.2 ± 3.1 (649)	100 (719)
daf-1(m213); smoc-1(tm7125) #2	0 (544)	99.4 ± 0.5 (676)	100 (378)

n, number of worms scored at each temperature, from a total of five plates per genotype assayed at each condition. For each double-mutant combination, two independent isolates (#1 and #2) were examined. % Daf-c, mean dauer formation percentage ± SD.

[a] $P < 0.05$, as calculated by an ANOVA and Tukey's honest significant difference, between a double mutant and the corresponding *daf* single mutant at the specified temperature.

pJKL1139[smoc-1 2 kb promoter::4xnls::gfp::unc-54 3′UTR] and generated integrated transgenic lines carrying this reporter (*jjIs4688* and *jjIs4694*, Table 1) for further analysis.

The integrated *smoc-1* transcriptional reporter showed strong GFP expression. GFP was first detectable in several cells located in the anterior of bean-stage embryos (Figure 6E). In the developing larvae, GFP is expressed in cells of the pharynx, the intestine, and the posterior hypodermis (Figure 6B). Pharyngeal cells expressing *smoc-1p::gfp* include the epithelial cells e2, the marginal cells mc1 and mc2, the M4 neuron, and all six of the pharyngeal/intestinal valve cells (Figure 6C). Cells of the posterior hypodermis expressing *smoc-1p::gfp* include hyp8, hyp9, hyp10, and hyp11 (Figure 6D). Expression in these tissues persisted from the L1 larval stage through adulthood. We noted that while all transgenic animals showed GFP expression in the pharynx and the posterior hypodermis, a small fraction of animals (~8%) did not exhibit GFP expression in all or some of the intestinal cells (Figure 6G). We observed no GFP expression in any other tissues, including the nerve cord, body wall muscles (BWMs), or the M lineage. Thus, *smoc-1* is expressed in cells of the pharynx, intestine, and posterior hypodermis.

Intestinal expression of smoc-1 is positively regulated by BMP signaling

We next asked whether *smoc-1* expression is regulated by the BMP pathway or by SMOC-1 itself. We introduced the integrated *smoc-1* transgenic reporter into BMP pathway null mutants, including *sma-3(jj3)*, *sma-6(jj1)*, *lon-2(e678)*, and *smoc-1(tm7125)* mutants (Table 1), and examined the expression pattern of the GFP reporter. Intriguingly, while the expression pattern and expression level of the GFP reporter in the pharynx and posterior hypodermis remained relatively constant in all mutant backgrounds examined, in *sma-6(jj1)* and *sma-3(jj3)* mutants there was a significant decrease in the percentage of animals that exhibited GFP expression in the intestinal cells, and a decrease in the intensity of intestinal GFP expression compared with WT animals (Figure 6, F and G). There was also a moderate decrease in the percentage of animals showing intestinal GFP expression in *smoc-1(tm7125)* mutants (Figure 6G). In contrast, nearly 100% of *lon-2(e678)* animals showed bright intestinal GFP expression, as compared to ~92% for WT animals (Figure 6G). Collectively, these results suggest that *smoc-1* expression in the intestinal cells is positively regulated by BMP signaling.

We have shown that *smoc-1(OE)*; *dbl-1(ok3749)* double mutants are as small as *dbl-1(ok3749)* single mutants (Figure 4B). Since expression of the *smoc-1* transcriptional reporter is significantly reduced in intestinal cells of *dbl-1(ok3749)* mutants, it is possible that the small body size phenotype of *smoc-1(OE)*; *dbl-1(ok3749)* double mutants is due to insufficient levels of *smoc-1* expression in the *dbl-1(ok3749)* background. To address this question, we generated a new construct *pJKL1217[dpy-30p::smoc-1 cDNA::unc-54 3′UTR]* (Table 2), which drives ubiquitous *smoc-1* expression under the control of the *dpy-30* promoter. DPY-30 is an essential component of the *C. elegans* dosage compensation machinery (Hsu and Meyer 1994; Hsu *et al.* 1995), and *dpy-30* expression is not known to be regulated by BMP signaling. We found that WT worms carrying the *[dpy-30p::smoc-1 cDNA::unc-54 3′UTR]* transgene are longer than WT worms (Figure 4, C and D), just like the *smoc-1(OE)* strain described above. However, *dbl-1(ok3749)* mutants carrying the *[dpy-30p::smoc-1 cDNA::unc-54 3′UTR]* transgene are as small as *dbl-1(ok3749)* single mutants (Figure 4, E and F). These findings demonstrate that SMOC-1 functions in a positive feedback loop to promote BMP signaling: SMOC-1 acts through the DBL-1/BMP ligand and its downstream Smad proteins to promote BMP signaling, while BMP signaling itself positively promotes the expression of *smoc-1* in intestinal cells.

smoc-1 functions cell nonautonomously to regulate body size and M-lineage development

The *smoc-1* transcriptional reporters identified cells in the pharynx, intestine, and posterior hypodermis as *smoc-1*-expressing cells. To determine in which tissue(s) expression of *smoc-1* is sufficient to regulate BMP signaling, we used a set of promoters to drive *smoc-1* cDNA in a tissue-specific

Table 5 LON-2 does not play a significant role in the TGFβ dauer pathway

Genotype	15°C % Daf-c (*n*)	20°C % Daf-c (*n*)	25°C % Daf-c (*n*)
lon-2(e678)	0 (807)	0 (799)	0 (1090)
daf-7(e1372)	22.7 ± 32.1 (141)	83.3 ± 6.5 (257)	100 (357)
daf-7(e1372); lon-2(e678)) #1	25.3 ± 8.7 (435)	59.4 ± 16.4 (239)[a]	100 (749)
daf-7(e1372); lon-2(e678) #2	31.7 ± 4.8 (249)	66.7 ± 11.7 (426)	100 (840)
daf-1(m213)	0.3 ± 1.0 (313)	97.9 ± 26.0 (570)	100 (853)
daf-1(m213); lon-2(e678) #1	0.2 ± 0.3 (575)	92.1 ± 2.9 (643)	100 (1149)
daf-1(m213); lon-2(e678) #2	0.5 ± 0.8 (654)	77.7 ± 5.0 (515)	100 (832)

n, number of worms scored at each temperature; from a total of five plates per genotype assayed at each condition. For each double-mutant combination, two independent isolates (#1 and #2) were examined. % Daf-c, mean dauer formation percentage ± SD.

[a] $P < 0.05$, as calculated by an ANOVA and Tukey's honest significant difference, between a double mutant and the corresponding *daf* single mutant at the specified temperature.

manner, and assayed for rescue of the *smoc-1(tm7125)* mutant phenotypes. Each construct was introduced into *smoc-1(tm7125)* worms for the body size assay, and into *smoc-1(tm7125)*; *sma-9(cc604)* worms for the Susm assay.

As shown in Figure 7A, forced expression of *smoc-1* cDNA specifically within each individual *smoc-1*-expressing tissue [driven by *ifb-2p* for intestinal cells (Hüsken *et al.* 2008) or *elt-3p* for hypodermal cells (Gilleard *et al.* 1999)] not only rescued the small body size of *smoc-1(tm7125)* mutants, but also made the transgenic worms longer, just like *smoc-1* cDNA under the control of its own promoter. Forced expression of *smoc-1* cDNA in tissues that do not express *smoc-1* [driven by *myo-2p* for pharyngeal muscles (Okkema *et al.* 1993), *myo-3p* for BWMs (Okkema *et al.* 1993), or *rab-3p* for pan neurons (Nonet *et al.* 1997)] also rescued the small body size of *smoc-1(tm7125)* mutants, and made the transgenic worms longer (Figure 7A). An exception is the lack of rescue of the body size phenotype in *smoc-1(tm7125)* mutants upon forced expression of *smoc-1* cDNA in the M lineage using the *hlh-8* promoter (Harfe *et al.* 1998). This could be due to the transient nature of *hlh-8* promoter activity in undifferentiated M-lineage cells during larval development (Harfe *et al.* 1998). We also crossed the *[myo-2p*::*smoc-1 cDNA*::*unc-54 3′UTR]* transgene into *dbl-1(ok3749)* mutants. As shown in Figure 7B, the same transgene *[myo-2p*::*smoc-1 cDNA*::*unc-54 3′UTR]* that caused a longer body size in *smoc-1(tm7125)* mutants did not increase the body size of *dbl-1(ok3749)* mutants. These observations, together with data presented in Figure 4, firmly establish that SMOC-1's function in regulating body size is dependent on the BMP ligand DBL-1.

Similar to the body size rescue results, forced expression of *smoc-1* cDNA in both *smoc-1*-expressing cells (intestine or hypodermis) and cells that do not normally express *smoc-1* (pharyngeal muscles, BWMs, pan neurons, or the M lineage) rescued the Susm phenotype of *smoc-1(tm7125)* mutants (Figure 7B), although for reasons currently unknown, the rescuing efficiency appeared lower when *smoc-1* expression was forced in BWMs or neurons (Figure 7C). Taken together, our results demonstrate that SMOC-1 can function cell non-autonomously to regulate both body size and M-lineage patterning. This is consistent with SMOC-1 being a putative secreted protein.

Human SMOC proteins can partially rescue the smoc-1(0) mutant phenotype in C. elegans

As described above, SMOC-1 has two human homologs, SMOC1 (hSMOC1) and SMOC2 (hSMOC2). We next asked whether either of the human SMOCs can substitute for SMOC-1 function in *C. elegans*. We first generated plasmids by directly putting the coding region of hSMOC1 or hSMOC2 in between the 2-kb *smoc-1* promoter and the *unc-54* 3′-UTR (Figure 8A and Table 2), and tested their functionality using the Susm assay. Neither hSMOC1 nor hSMOC2 rescued the Susm phenotype of *smoc-1(tm7125)* worms (Figure 8B). We reasoned that the lack of rescue may be due to differences in the signal peptide between humans and *C. elegans*, causing the proteins to not be properly secreted from cells (Tian *et al.* 2010). We next generated plasmids expressing chimeric SMOC proteins that have the worm SMOC-1 signal peptide (CelSP) followed by the extracellular region of hSMOC1 or hSMOC2 (Figure 8A and Table 2). Both CelSP::hSMOC1 and CelSP::hSMOC2 partially rescued the Susm phenotype of *smoc-1(tm7125)* mutants (Figure 8B), but failed to rescue the body size phenotype (Figure 8C). Nevertheless, these results demonstrate that CelSP:hSMOC1 and CelSP:hSMOC2 can function to regulate BMP signaling in *C. elegans*, and suggest that the function of SMOC proteins in regulating BMP signaling is evolutionarily conserved from worms to humans.

Discussion

In this study, we identified the sole SMOC protein in *C. elegans*, which belongs to the SPARC/BM40 family of matricellular proteins, as a key player in the BMP signaling pathway. *smoc-1(0)* mutations cause a reduction in body size and suppress the *sma-9(0)* M-lineage defect, but *smoc-1(0)* mutants are not as small as null mutants in core components of the BMP pathway (Figure 1, Figure 2, Figure 3, and Table 3). These phenotypes resemble those caused by mutations in other modulators of the BMP pathway, such as DRAG-1/RGM (Tian *et al.* 2010), TSP-21 (Liu *et al.* 2015), or SUP-17/ADAM10 (Wang *et al.* 2017), and are consistent with a modulatory role for SMOC-1 in the BMP pathway. Over- or

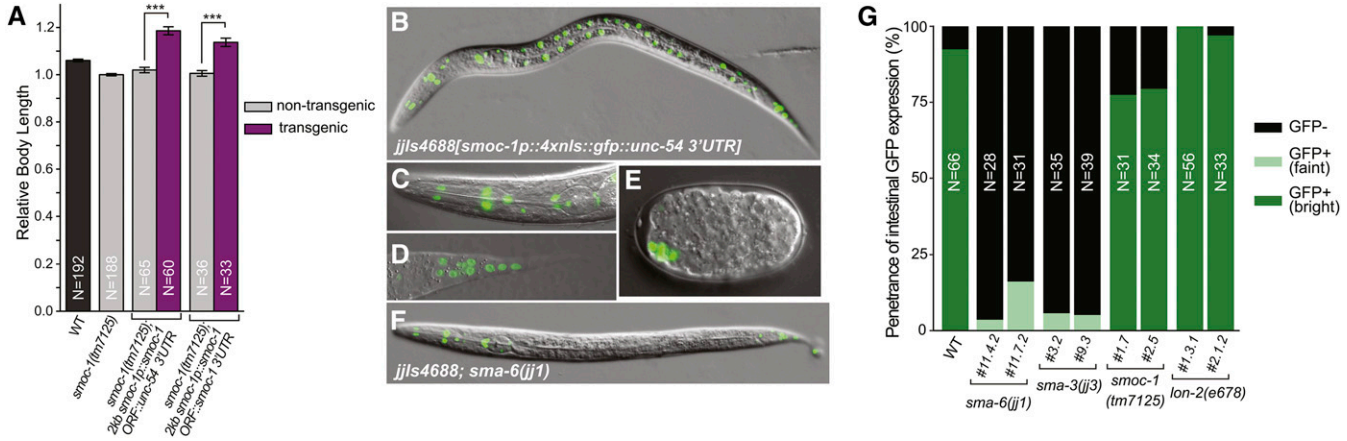

Figure 6 *smoc-1* is expressed in multiple tissues and its intestinal expression is positively regulated by BMP signaling. (A) Expression of *smoc-1* cDNA under different regulatory elements to test for rescue of the body size phenotype of *smoc-1(tm7125)* worms. For each construct, two independent transgenic lines were examined, and the data were combined and averaged. Body sizes are relative to *smoc-1(tm7125)* mutant worms (set to 1.0) and all measurements were done on the same day. Error bars represent 95% C.I. *** $P < 0.0001$. (B–F) Merged GFP and DIC images of WT worms (B–E) and a *sma-6(jj1)* mutant worm (F) carrying the integrated *smoc-1* transcriptional reporter *jjIs4688* (Table 1). In WT embryos, GFP expression is detectable at the bean stage (E). In developing WT larvae, GFP expression is detectable in the pharynx (B and C), intestine (B), and posterior hypodermis (B and D). GFP expression in the intestine, but not in the pharynx or posterior hypodermis, is significantly reduced in *sma-6(jj1)* larvae (F). Images are side views with anterior to the left and dorsal up. (G) Proportions of WT and mutant worms with intestinal expression of the *smoc-1* transcriptional reporter. Two independent isolates were assessed for each gene tested. WT, wild-type.

ectopic expression of *smoc-1* led to a significant increase in body size, and an increase in RAD-SMAD reporter expression. Moreover, the long body size phenotype caused by *smoc-1(OE)* is completely suppressed by null mutations in the BMP ligand DBL-1 and the R-Smad SMA-3 (Figure 4 and Figure 7B). Collectively, these findings demonstrate that SMOC-1 functions through the BMP ligand DBL-1 and acts as a positive modulator to promote BMP signaling. Importantly, the expression of *smoc-1* in the intestine is positively regulated by BMP signaling (Figure 6). Thus, SMOC-1 functions in a positive feedback loop in the BMP pathway. We speculate that this mode of feedback regulation ensures robustness of BMP signaling.

How might SMOC-1 function to promote BMP signaling? Our tissue-specific rescue data coupled with the expression pattern of *smoc-1* (Figure 6 and Figure 7) showed that SMOC-1 functions cell nonautonomously to regulate BMP signaling. This is consistent with SMOC-1 being a predicted secreted protein. Strikingly, forced expression of *smoc-1* exclusively in pharyngeal muscles is sufficient to rescue both the body size and the Susm phenotype of *smoc-1(0)* mutants (Figure 7). Notably, the M-lineage cells, where the Smad proteins function to regulate M-lineage development (Foehr *et al.* 2006), are located in the posterior of a developing larva, distant from the pharynx. Thus, SMOC-1 can function over long distances, from a source located far from BMP-receiving cells, to regulate the output of BMP signaling.

The *Drosophila* homolog of SMOC-1, Pent, can also function over long distances to regulate Dpp/BMP signaling in the developing wing imaginal discs (Vuilleumier *et al.* 2010). In particular, Pent has been shown to bind to and induce the internalization of the BMP coreceptor Dally/glypican [a heparan sulfate proteoglycan (HSPG)], such that the trapping of Dpp/BMP by Dally is reduced, which in turn promotes the spreading of Dpp/BMP (Norman *et al.* 2016). Using a *Xenopus* animal cap transfer assay, Thomas and colleagues (Thomas *et al.* 2017) showed that *Xenopus* SMOC-1 can also expand the range of BMP signaling by competing with BMP to bind to HSPGs. In *C. elegans*, the glypican homolog LON-2 is a known negative regulator of BMP signaling. LON-2 can bind to BMP *in vitro*, and has been proposed to function in the signal-receiving cells, the hypodermal cells, to negatively regulate BMP signaling by sequestering the DBL-1/BMP ligand (Gumienny *et al.* 2007). Our genetic analysis between *lon-2(0)* and *smoc-1(0)* mutations suggests that SMOC-1 antagonizes the function of LON-2 in regulating BMP signaling (Figure 5A). How SMOC-1 and LON-2 can functionally antagonize each other is currently unknown. One possible model is that the two proteins function completely independently to regulate BMP signaling. Alternatively, based on the observed physical interaction between HSPG and the *Drosophila* and *Xenopus* SMOC homologs, one can envision that SMOC-1 may promote BMP signaling by binding to LON-2/glypican and inhibiting LON-2's ability to sequester the DBL-1/BMP ligand. However, SMOC-1 must have LON-2/glypican-independent function(s), because *smoc-1(OE)* can further increase body size in the absence of LON-2/glypican, as in *smoc-1(OE)*; *lon-2(0)* double mutants shown in Figure 5B, and *smoc-1(0)*; *lon-2(0)* double mutants exhibit an intermediate body length between those of each single mutant.

The molecular mechanism underlying the LON-2/glypican-independent function of SMOC-1 is currently unknown. In addition to LON-2, there are five other HSPG-encoding genes in the *C. elegans* genome: *unc-52*, *cle-1*, *gpn-1*, *sdn-1*,

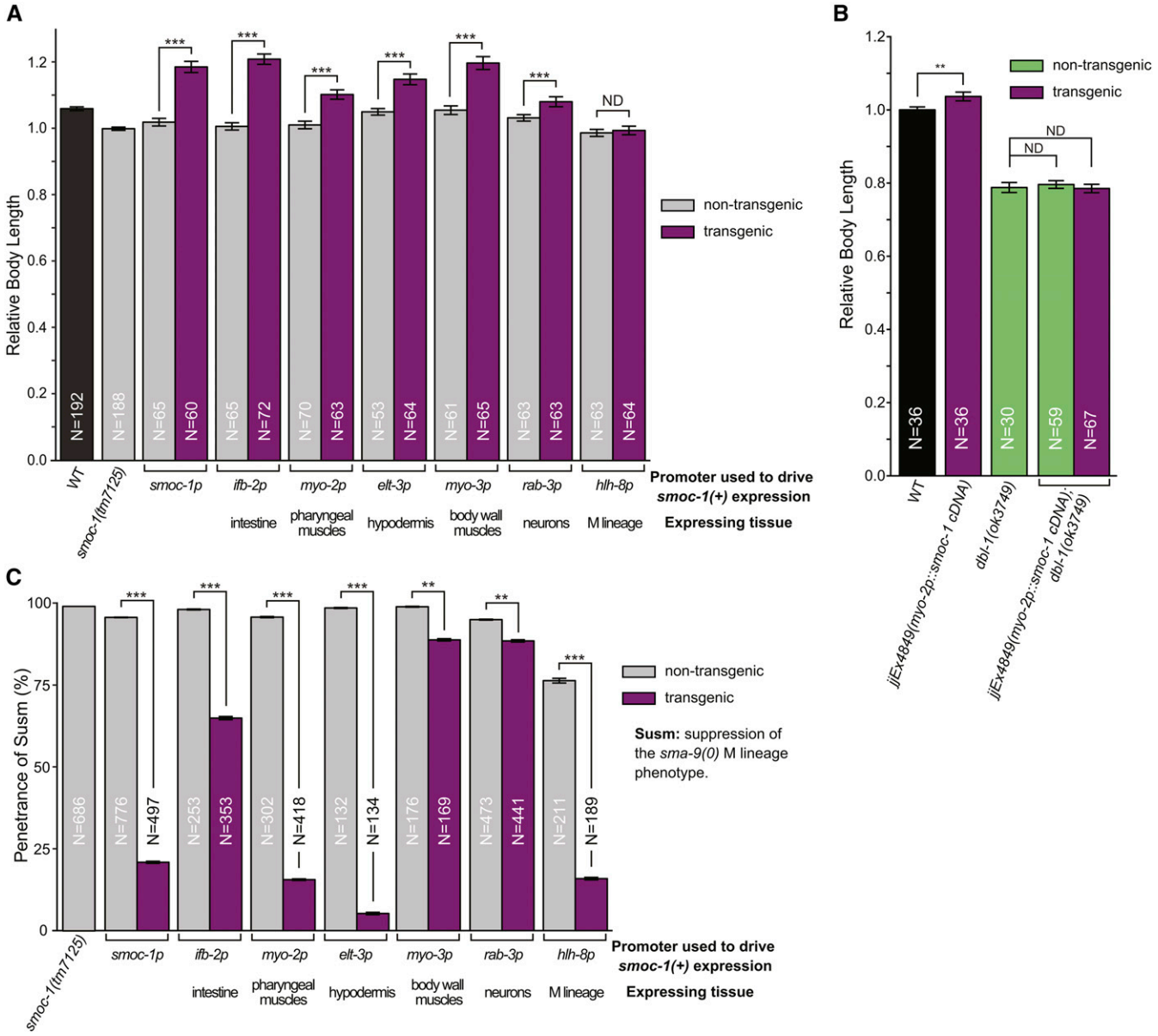

Figure 7 *smoc-1* functions cell nonautonomously to regulate body size and M-lineage development. Tissue-specific expression of *smoc-1* cDNA to test for rescue of the body size (A) or Susm (C) phenotype of *smoc-1(tm7125)* worms. *smoc-1* cDNA was driven by each specific promoter to allow expression in a given tissue. All constructs used the *unc-54* 3′-UTR. For each construct, two independent transgenic lines were examined and the measurements were averaged. (A) Body sizes are relative to *smoc-1(tm7125)* mutant worms (set to 1.0) and all measurements were done on the same day. (B) Relative body length of developmental stage-matched WT and *dbl-1(ok3749)* worms that either carry or do not carry the *jjEx4849[myo-2p*::*smoc-1 cDNA*::*unc-54 3′UTR]* transgene. Body sizes are relative to WT worms (set to 1.0) and all measurements were done on the same day. (A and B) Error bars represent 95% C.I. An ANOVA followed by Tukey's honest significant difference was used to test for differences in body size between groups. (C) The Susm phenotype was scored in the background of *smoc-1(tm7125)*; *sma-9(cc604)*; *CC*::*gfp*. A Wald test was used to determine if transgenic state is associated with CC number. Error bars represent SE. ** $P < 0.001$ and *** $P < 0.0001$. CC, coelomocyte; ND, no difference; Susm, suppression of *sma-9(0)* M-lineage defect; WT, wild-type.

and *agr-1* (Rogalski *et al.* 1993; Halfter *et al.* 1998; Ackley *et al.* 2001; Rhiner *et al.* 2005; Hrus *et al.* 2007). It is possible that in addition to LON-2/glypican, one or multiple of these other HSPGs also functions with SMOC-1 to regulate BMP signaling. Alternatively, SMOC-1 may promote BMP signaling by interacting with other cell surface or extracellular BMP regulators, or even with DBL-1/BMP itself, to promote BMP signaling. Any LON-2/glypican-independent function of SMOC-1 still requires DBL-1/BMP, because *smoc-1(OE)*; *dbl-1(0)* double mutants are as small as *dbl-1(0)* null mutants. Our model, proposing that SMOC-1 has dual modes of action to regulate BMP signaling, is consistent with structure–function analysis of *Xenopus* SMOC-1 (XSMOC-1), whose EC domains can bind to HSPG and promote BMP

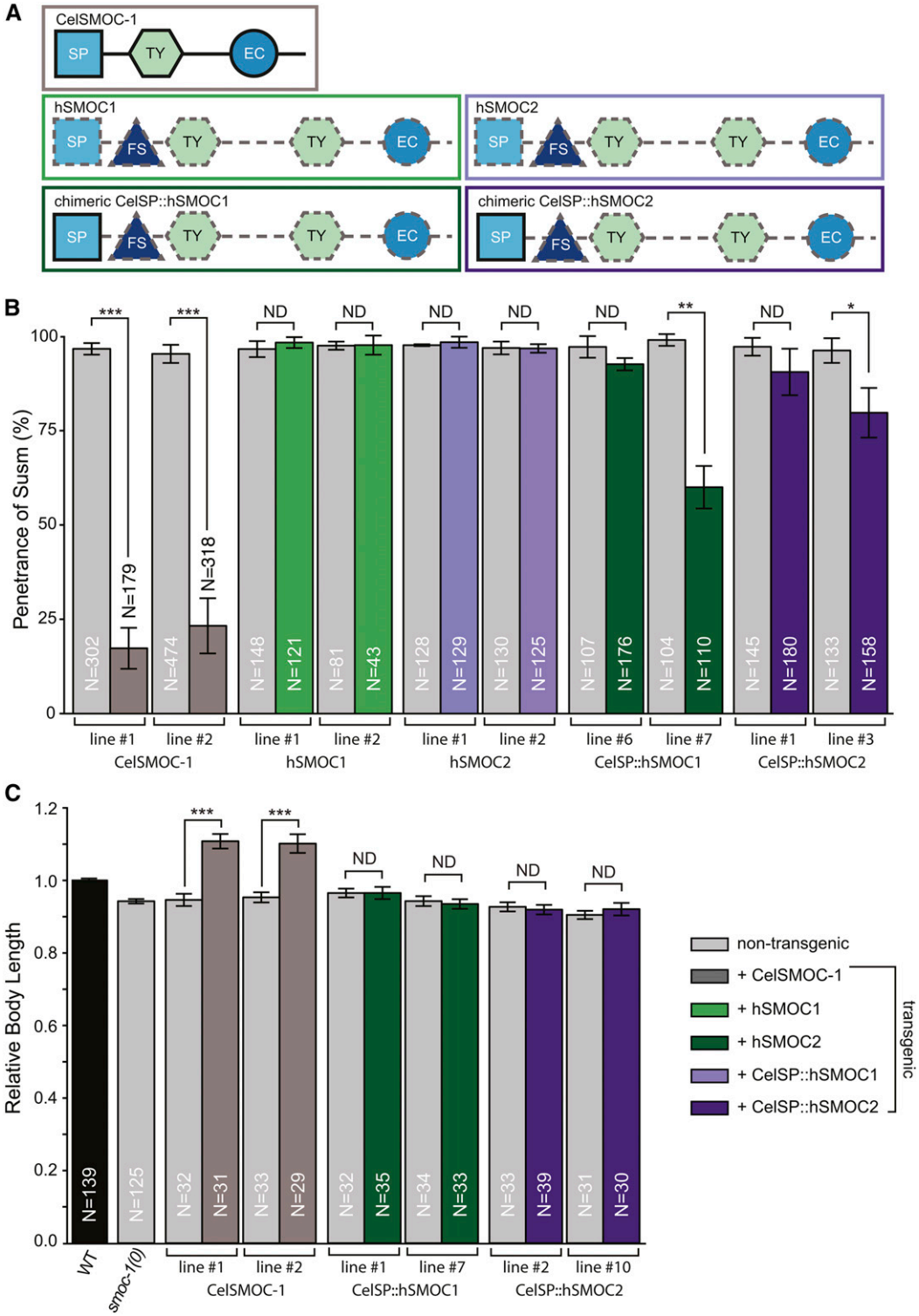

Figure 8 Human SMOC proteins can partially rescue the Susm phenotype of *smoc-1(0)* mutants. (A) Schematics of SMOC homologs tested for function in *C. elegans*. Solid black outline indicates *C. elegans* protein sequences. Dashed gray line indicates human protein sequences. All ORFs were cloned into the same vector with the same regulatory elements (2-kb *smoc-1* promoter and *unc-54* 3′-UTR), and each construct was tested for the rescue of Susm (B) and body size (C) phenotype of *smoc-1(tm7125)* mutants. Two independent lines were assayed for each construct. (B) The Susm phenotype was scored in the background of *smoc-1(tm7125)*; *sma-9(cc604)*; *CC::gfp*. A Wald test was used to determine if transgenic state is associated with CC number. Error bars represent SE. (C) Body sizes are relative to WT worms (set to 1.0), and all measurements were done on the same day. An ANOVA followed by Tukey's honest significant difference was used to test for differences between groups. Error bars represent 95% C.I. * $P < 0.01$, ** $P < 0.001$, and *** $P < 0.0001$. CC, coelomocyte; EC, secreted protein acidic and rich in cysteine (SPARC) extracellular calcium-binding domain; FS, follistatin-like domain; ND, no difference; SP, signal peptide; Susm, suppression of *sma-9(0)* M-lineage defect; TY, thyroglobulin type I-like repeat WT, wild-type.

spreading, while the TY domains are necessary for XSMOC-1 to inhibit BMP signaling (Thomas *et al.* 2017). We have shown that both the TY and EC domains in *C. elegans* SMOC-1 are important for its function in BMP signaling, because mutations in either domain disrupt the function of SMOC-1 (Figure 2). Further dissection of the roles of each of these domains at the molecular level will help clarify the mechanisms underlying SMOC-1 function in the BMP pathway.

In this study, we have shown that in addition to being a positive regulator of BMP signaling, *smoc-1* is also positively regulated by BMP signaling at the transcriptional level (Figure 6). In *Drosophila*, *Pent* transcription is directly regulated by BMP signaling via the silencer elements that are bound by the Smad-Shn repressive complex (Vuilleumier *et al.* 2010). Whether *smoc-1* is directly or indirectly regulated by BMP signaling in *C. elegans* remains to be determined. Nevertheless, our results suggest a model in which SMOC-1 functions in a positive feedback loop to regulate BMP signaling (Figure 9). We argue that this mode of regulatory relationship between SMOC-1 and the BMP pathway ensures robustness of BMP signaling in processes that require high levels of BMP signaling. Consistent with this notion, *smoc-1(0)* mutants exhibit a smaller body size, but do not appear to have major defects in the male tail, a process previously known to require a lower threshold of BMP signaling (Krishna *et al.* 1999).

Human SMOC1 can bind to the TGFβ coreceptor endoglin to regulate TGFβ signaling in endothelial cells (Awwad *et al.* 2015). Our genetic analysis suggests that SMOC-1 does not play a key role, but may play a minor or modulatory role, in regulating the TGFβ-like dauer pathway in *C. elegans* (Table 4). Because the BMP pathway and the TGFβ-like dauer pathway share DAF-4 as the sole type II receptor in *C. elegans*, there might be low levels of cross talk between these two pathways, which has been previously documented for other BMP pathway mutations (Krishna *et al.* 1999; Maduzia *et al.* 2005; Tian *et al.* 2010).

In addition to their roles in regulating BMP signaling, SMOC-1 homologs have also been found to function in other signaling pathways. Pent has been shown to play a role in regulating Wg signaling in the *Drosophila* wing (Norman *et al.* 2016). SMOC2 can potentiate endothelial growth factor or fibroblast growth factor activity to promote angiogenesis in cultured human umbilical vein endothelial cells (Rocnik *et al.* 2006). Whether SMOC-1 is involved in other signaling pathways in *C. elegans* is currently unknown.

There are two SMOC homologs in mammals. SMOC1 is essential for eye and limb development in mice, and mutations in SMOC1 in humans cause microphthalmia with limb anomalies and ophthalmo-acromelic syndrome (also known as Waardenburg anophthalmia syndrome), both of which affect eye and limb development (Okada *et al.* 2011; Rainger *et al.* 2011). Mutations in hSMOC2 have also been found to be associated with defects in dental development (Bloch-Zupan *et al.* 2011; Alfawaz *et al.* 2013) and vitiligo (Alkhateeb *et al.* 2010; Birlea *et al.* 2010). QTL mapping in different dog breeds has found that a retrotransposon insertion that disrupts SMOC2 splicing and reduces its expression is associated with canine brachycephaly (Marchant *et al.* 2017). In addition, several different types of brain tumors exhibit altered expression of SMOC1 (Brellier *et al.* 2011), while SMOC2 is an intestinal stem cell signature gene (Muñoz *et al.* 2012) that is required for L1-mediated colon cancer progression (Shvab *et al.* 2016). Notably, BMP signaling is known to play important roles in eye, tooth, and limb development, and abnormal BMP signaling can cause cancer (Thawani *et al.* 2010). Here, we have demonstrated that both hSMOC1 and hSMOC2 can partially rescue the Susm phenotype of *smoc-1(0)* mutants (Figure 8), suggesting that the function of SMOC proteins in regulating BMP signaling is evolutionarily conserved. Future studies on how SMOC-1 functions to regulate BMP signaling in an *in vivo* system such as *C. elegans* may have implications for human health.

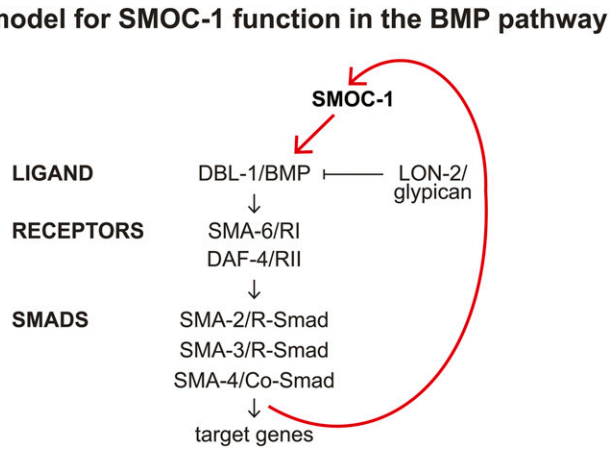

Figure 9 A model for SMOC-1 function in the BMP pathway to regulate body size. SMOC-1 acts through the BMP ligand DBL-1/BMP, and in part by antagonizing LON-2/glypican, to promote BMP signaling. BMP signaling in turn promotes the intestinal expression of *smoc-1*, thus creating a positive feedback loop. Red lines do not imply direct interaction.

Acknowledgments

We thank Oliver Hobert and Shohei Mitani for plasmids and strains, Peter Okkema for help with identifying cells located in the pharynx, Florencia Schlamp for advice on data analysis using R, Erich Schwarz for mining the Model Organism ENCyclopedia of DNA Elements data, Gabriela Rojas for help generating the *smoc-1(OE)*; *RAD-SMAD* strains, and the rest of the Liu laboratory for critical comments and suggestions. Some strains were obtained from the *Caenorhabditis* Genetics Center, which is funded by National Institutes of Health (NIH) Office of 27 Research Infrastructure Programs (P40 OD-010440). This study was supported by NIH grants R01 GM-066953 and R01 GM-103869 to J.L. M.S.D. was partially supported by an NIH Predoctoral Training Grant (T32 GM-007617), a Dean's Excellence Fellowship from the Cornell Graduate School, and a

National Science Foundation (NSF) Graduate Research Fellowship (DGE-1650441). A.E. was a student in the Molecular Biology and Genetics Research Experience for Undergraduate (MBG-REU) program, which was supported by the NSF (DBI1659534), the Department of Molecular Biology and Genetics, the Weill Institute of Cell and Molecular Biology, and the Division of Nutritional Sciences at Cornell University. A.N.M. was a Hunter R. Rawlings III Presidential Research Scholar at Cornell University.

Literature Cited

Ackley, B. D., J. R. Crew, H. Elamaa, T. Pihlajaniemi, C. J. Kuo *et al.*, 2001 The NC1/endostatin domain of Caenorhabditis elegans type XVIII collagen affects cell migration and axon guidance. J. Cell Biol. 152: 1219–1232. https://doi.org/10.1083/jcb.152.6.1219

Alfawaz, S., F. Fong, V. Plagnol, F. S. Wong, J. Fearne *et al.*, 2013 Recessive oligodontia linked to a homozygous loss-of-function mutation in the SMOC2 gene. Arch. Oral Biol. 58: 462–466. https://doi.org/10.1016/j.archoralbio.2012.12.008

Alkhateeb, A., N. Al-Dain Marzouka, and F. Qarqaz, 2010 SMOC2 gene variant and the risk of vitiligo in Jordanian Arabs. Eur. J. Dermatol. 20: 701–704. https://doi.org/10.1684/ejd.2010.1095

Awwad, K., J. Hu, L. Shi, N. Mangels, R. Abdel Malik *et al.*, 2015 Role of secreted modular calcium-binding protein 1 (SMOC1) in transforming growth factor beta signalling and angiogenesis. Cardiovasc. Res. 106: 284–294. https://doi.org/10.1093/cvr/cvv098

Birlea, S. A., K. Gowan, P. R. Fain, and R. A. Spritz, 2010 Genome-wide association study of generalized vitiligo in an isolated European founder population identifies SMOC2, in close proximity to IDDM8. J. Invest. Dermatol. 130: 798–803. https://doi.org/10.1038/jid.2009.347

Bloch-Zupan, A., X. Jamet, C. Etard, V. Laugel, J. Muller *et al.*, 2011 Homozygosity mapping and candidate prioritization identify mutations, missed by whole-exome sequencing, in SMOC2, causing major dental developmental defects. Am. J. Hum. Genet. 89: 773–781. https://doi.org/10.1016/j.ajhg.2011.11.002

Bradshaw, A. D., 2012 Diverse biological functions of the SPARC family of proteins. Int. J. Biochem. Cell Biol. 44: 480–488. https://doi.org/10.1016/j.biocel.2011.12.021

Bragdon, B., O. Moseychuk, S. Saldanha, D. King, J. Julian *et al.*, 2011 Bone morphogenetic proteins: a critical review. Cell. Signal. 23: 609–620. https://doi.org/10.1016/j.cellsig.2010.10.003

Brazil, D. P., R. H. Church, S. Surae, C. Godson, and F. Martin, 2015 BMP signalling: agony and antagony in the family. Trends Cell Biol. 25: 249–264. https://doi.org/10.1016/j.tcb.2014.12.004

Brellier, F., S. Ruggiero, D. Zwolanek, E. Martina, D. Hess *et al.*, 2011 SMOC1 is a tenascin-C interacting protein over-expressed in brain tumors. Matrix Biol. 30: 225–233. https://doi.org/10.1016/j.matbio.2011.02.001

Brenner, S., 1974 The genetics of Caenorhabditis elegans. Genetics 77: 71–94.

Busch, E., E. Hohenester, R. Timpl, M. Paulsson, and P. Maurer, 2000 Calcium affinity, cooperativity, and domain interactions of extracellular EF-hands present in BM-40. J. Biol. Chem. 275: 25508–25515. https://doi.org/10.1074/jbc.M001770200

Estevez, M., L. Attisano, J. L. Wrana, P. S. Albert, J. Massague *et al.*, 1993 The daf-4 gene encodes a bone morphogenetic protein receptor controlling C. elegans dauer larva development. Nature 365: 644–649. https://doi.org/10.1038/365644a0

Finn, R. D., T. K. Attwood, P. C. Babbitt, A. Bateman, P. Bork *et al.*, 2017 InterPro in 2017-beyond protein family and domain annotations. Nucleic Acids Res. 45: D190–d199. https://doi.org/10.1093/nar/gkw1107

Foehr, M. L., A. S. Lindy, R. C. Fairbank, N. M. Amin, M. Xu *et al.*, 2006 An antagonistic role for the C. elegans Schnurri homolog SMA-9 in modulating TGFbeta signaling during mesodermal patterning. Development 133: 2887–2896. https://doi.org/10.1242/dev.02476

Georgi, L. L., P. S. Albert, and D. L. Riddle, 1990 daf-1, a C. elegans gene controlling dauer larva development, encodes a novel receptor protein kinase. Cell 61: 635–645. https://doi.org/10.1016/0092-8674(90)90475-T

Gilleard, J. S., Y. Shafi, J. D. Barry, and J. D. McGhee, 1999 ELT-3: a Caenorhabditis elegans GATA factor expressed in the embryonic epidermis during morphogenesis. Dev. Biol. 208: 265–280. https://doi.org/10.1006/dbio.1999.9202

Gumienny, T. L., and C. Savage-Dunn, 2013 TGF-beta signaling in C. elegans (July 10, 2013), WormBook, ed. The C. elegans Research Community WormBook, doi/10.1895/wormbook.1.22.2, http://www.wormbook.org. https://doi.org/10.1895/wormbook.1.22.2

Gumienny, T. L., L. T. MacNeil, H. Wang, M. de Bono, J. L. Wrana *et al.*, 2007 Glypican LON-2 is a conserved negative regulator of BMP-like signaling in Caenorhabditis elegans. Curr. Biol. 17: 159–164. https://doi.org/10.1016/j.cub.2006.11.065

Halfter, W., S. Dong, B. Schurer, and G. J. Cole, 1998 Collagen XVIII is a basement membrane heparan sulfate proteoglycan. J. Biol. Chem. 273: 25404–25412. https://doi.org/10.1074/jbc.273.39.25404

Harfe, B. D., A. Vaz Gomes, C. Kenyon, J. Liu, M. Krause *et al.*, 1998 Analysis of a Caenorhabditis elegans twist homolog identifies conserved and divergent aspects of mesodermal patterning. Genes Dev. 12: 2623–2635. https://doi.org/10.1101/gad.12.16.2623

Hohenester, E., P. Maurer, C. Hohenadl, R. Timpl, J. N. Jansonius *et al.*, 1996 Structure of a novel extracellular Ca(2+)-binding module in BM-40. Nat. Struct. Biol. 3: 67–73. https://doi.org/10.1038/nsb0196-67

Hrus, A., G. Lau, H. Hutter, S. Schenk, J. Ferralli *et al.*, 2007 C. elegans agrin is expressed in pharynx, IL1 neurons and distal tip cells and does not genetically interact with genes involved in synaptogenesis or muscle function. PLoS One 2: e731. https://doi.org/10.1371/journal.pone.0000731

Hsu, D. R., and B. J. Meyer, 1994 The dpy-30 gene encodes an essential component of the Caenorhabditis elegans dosage compensation machinery. Genetics 137: 999–1018.

Hsu, D. R., P. T. Chuang, and B. J. Meyer, 1995 DPY-30, a nuclear protein essential early in embryogenesis for Caenorhabditis elegans dosage compensation. Development 121: 3323–3334.

Hüsken, K., T. Wiesenfahrt, C. Abraham, R. Windoffer, O. Bossinger *et al.*, 2008 Maintenance of the intestinal tube in Caenorhabditis elegans: the role of the intermediate filament protein IFC-2. Differentiation 76: 881–896. https://doi.org/10.1111/j.1432-0436.2008.00264.x

Katagiri, T., and T. Watabe, 2016 Bone morphogenetic proteins. Cold Spring Harb. Perspect. Biol. 8: a021899. https://doi.org/10.1101/cshperspect.a021899

Krishna, S., L. L. Maduzia, and R. W. Padgett, 1999 Specificity of TGFbeta signaling is conferred by distinct type I receptors and their associated SMAD proteins in Caenorhabditis elegans. Development 126: 251–260.

Liang, J., R. Lints, M. L. Foehr, R. Tokarz, L. Yu *et al.*, 2003 The Caenorhabditis elegans schnurri homolog sma-9 mediates stage- and cell type-specific responses to DBL-1 BMP-related

signaling. Development 130: 6453–6464. https://doi.org/10.1242/dev.00863

Liu, Z., H. Shi, L. C. Szymczak, T. Aydin, S. Yun *et al.*, 2015 Promotion of bone morphogenetic protein signaling by tetraspanins and glycosphingolipids. PLoS Genet. 11: e1005221. https://doi.org/10.1371/journal.pgen.1005221

Lowery, J. W., B. Brookshire, and V. Rosen, 2016 A survey of strategies to modulate the bone morphogenetic protein signaling pathway: current and future perspectives. Stem Cells Int. 2016: 7290686. https://doi.org/10.1155/2016/7290686

Maduzia, L. L., A. F. Roberts, H. Wang, X. Lin, L. J. Chin *et al.*, 2005 C. elegans serine-threonine kinase KIN-29 modulates TGFbeta signaling and regulates body size formation. BMC Dev. Biol. 5: 8. https://doi.org/10.1186/1471-213X-5-8

Marchant, T. W., E. J. Johnson, L. McTeir, C. I. Johnson, A. Gow *et al.*, 2017 Canine brachycephaly is associated with a retrotransposon-mediated missplicing of SMOC2. Curr. Biol. 27: 1573–1584.e6. https://doi.org/10.1016/j.cub.2017.04.057

Mello, C. C., J. M. Kramer, D. Stinchcomb, and V. Ambros, 1991 Efficient gene transfer in C.elegans: extrachromosomal maintenance and integration of transforming sequences. EMBO J. 10: 3959–3970. https://doi.org/10.1002/j.1460-2075.1991.tb04966.x

Mok, D. Z., P. W. Sternberg, and T. Inoue, 2015 Morphologically defined sub-stages of C. elegans vulval development in the fourth larval stage. BMC Dev. Biol. 15: 26. https://doi.org/10.1186/s12861-015-0076-7

Morita, K., K. L. Chow, and N. Ueno, 1999 Regulation of body length and male tail ray pattern formation of Caenorhabditis elegans by a member of TGF-beta family. Development 126: 1337–1347.

Morita, K., A. J. Flemming, Y. Sugihara, M. Mochii, Y. Suzuki *et al.*, 2002 A Caenorhabditis elegans TGF-beta, DBL-1, controls the expression of LON-1, a PR-related protein, that regulates polyploidization and body length. EMBO J. 21: 1063–1073. https://doi.org/10.1093/emboj/21.5.1063

Muñoz, J., D. E. Stange, A. G. Schepers, M. van de Wetering, B. K. Koo *et al.*, 2012 The Lgr5 intestinal stem cell signature: robust expression of proposed quiescent '+4' cell markers. EMBO J. 31: 3079–3091. https://doi.org/10.1038/emboj.2012.166

Nonet, M. L., J. E. Staunton, M. P. Kilgard, T. Fergestad, E. Hartwieg *et al.*, 1997 Caenorhabditis elegans rab-3 mutant synapses exhibit impaired function and are partially depleted of vesicles. J. Neurosci. 17: 8061–8073. https://doi.org/10.1523/JNEUROSCI.17-21-08061.1997

Norman, M., R. Vuilleumier, A. Springhorn, J. Gawlik, and G. Pyrowolakis, 2016 Pentagone internalises glypicans to fine-tune multiple signalling pathways. Elife 5: e13301. https://doi.org/10.7554/eLife.13301

Okada, I., H. Hamanoue, K. Terada, T. Tohma, A. Megarbane *et al.*, 2011 SMOC1 is essential for ocular and limb development in humans and mice. Am. J. Hum. Genet. 88: 30–41. https://doi.org/10.1016/j.ajhg.2010.11.012

Okkema, P. G., S. W. Harrison, V. Plunger, A. Aryana, and A. Fire, 1993 Sequence requirements for myosin gene expression and regulation in Caenorhabditis elegans. Genetics 135: 385–404.

Rainger, J., E. van Beusekom, J. K. Ramsay, L. McKie, L. Al-Gazali *et al.*, 2011 Loss of the BMP antagonist, SMOC-1, causes ophthalmo-acromelic (Waardenburg Anophthalmia) syndrome in humans and mice. PLoS Genet. 7: e1002114. https://doi.org/10.1371/journal.pgen.1002114

R Core Team, 2015 *R: A Language and Environment for Statistical Computing*. R Foundation for Statistical Computing, Vienna.

Ren, P., C. S. Lim, R. Johnsen, P. S. Albert, D. Pilgrim *et al.*, 1996 Control of C. elegans larval development by neuronal expression of a TGF-beta homolog. Science 274: 1389–1391. https://doi.org/10.1126/science.274.5291.1389

Rhiner, C., S. Gysi, E. Frohli, M. O. Hengartner, and A. Hajnal, 2005 Syndecan regulates cell migration and axon guidance in C. elegans. Development 132: 4621–4633. https://doi.org/10.1242/dev.02042

Rocnik, E. F., P. Liu, K. Sato, K. Walsh, and C. Vaziri, 2006 The novel SPARC family member SMOC-2 potentiates angiogenic growth factor activity. J. Biol. Chem. 281: 22855–22864. https://doi.org/10.1074/jbc.M513463200

Rogalski, T. M., B. D. Williams, G. P. Mullen, and D. G. Moerman, 1993 Products of the unc-52 gene in Caenorhabditis elegans are homologous to the core protein of the mammalian basement membrane heparan sulfate proteoglycan. Genes Dev. 7: 1471–1484. https://doi.org/10.1101/gad.7.8.1471

Rual, J. F., J. Ceron, J. Koreth, T. Hao, A. S. Nicot *et al.*, 2004 Toward improving Caenorhabditis elegans phenome mapping with an ORFeome-based RNAi library. Genome Res. 14: 2162–2168. https://doi.org/10.1101/gr.2505604

Salazar, V. S., L. W. Gamer, and V. Rosen, 2016 BMP signalling in skeletal development, disease and repair. Nat. Rev. Endocrinol. 12: 203–221. https://doi.org/10.1038/nrendo.2016.12

Savage, C., P. Das, A. L. Finelli, S. R. Townsend, C. Y. Sun *et al.*, 1996 Caenorhabditis elegans genes sma-2, sma-3, and sma-4 define a conserved family of transforming growth factor beta pathway components. Proc. Natl. Acad. Sci. USA 93: 790–794. https://doi.org/10.1073/pnas.93.2.790

Savage-Dunn, C., and R. W. Padgett, 2017 The TGF-beta family in Caenorhabditis elegans. Cold Spring Harb. Perspect. Biol. 9: a022251.

Schindelin, J., I. Arganda-Carreras, E. Frise, V. Kaynig, M. Longair *et al.*, 2012 Fiji: an open-source platform for biological-image analysis. Nat. Methods 9: 676–682. https://doi.org/10.1038/nmeth.2019

Sedlmeier, G., and J. P. Sleeman, 2017 Extracellular regulation of BMP signaling: welcome to the matrix. Biochem. Soc. Trans. 45: 173–181. https://doi.org/10.1042/BST20160263

Shvab, A., G. Haase, A. Ben-Shmuel, N. Gavert, T. Brabletz *et al.*, 2016 Induction of the intestinal stem cell signature gene SMOC-2 is required for L1-mediated colon cancer progression. Oncogene 35: 549–557. https://doi.org/10.1038/onc.2015.127

Suzuki, Y., M. D. Yandell, P. J. Roy, S. Krishna, C. Savage-Dunn *et al.*, 1999 A BMP homolog acts as a dose-dependent regulator of body size and male tail patterning in Caenorhabditis elegans. Development 126: 241–250.

Thawani, J. P., A. C. Wang, K. D. Than, C. Y. Lin, F. La Marca *et al.*, 2010 Bone morphogenetic proteins and cancer: review of the literature. Neurosurgery 66: 233–246, discussion 246. https://doi.org/10.1227/01.NEU.0000363722.42097.C2

Thomas, J. T., D. Eric Dollins, K. R. Andrykovich, T. Chu, B. G. Stultz *et al.*, 2017 SMOC can act as both an antagonist and an expander of BMP signaling. Elife 6: e17935. https://doi.org/10.7554/eLife.17935

Tian, C., D. Sen, H. Shi, M. L. Foehr, Y. Plavskin *et al.*, 2010 The RGM protein DRAG-1 positively regulates a BMP-like signaling pathway in Caenorhabditis elegans. Development 137: 2375–2384. https://doi.org/10.1242/dev.051615

Tian, C., H. Shi, S. Xiong, F. Hu, W. C. Xiong *et al.*, 2013 The neogenin/DCC homolog UNC-40 promotes BMP signaling via the RGM protein DRAG-1 in C. elegans. Development 140: 4070–4080. https://doi.org/10.1242/dev.099838

Vannahme, C., N. Smyth, N. Miosge, S. Gosling, C. Frie *et al.*, 2002 Characterization of SMOC-1, a novel modular calcium-binding protein in basement membranes. J. Biol. Chem. 277: 37977–37986. https://doi.org/10.1074/jbc.M203830200

Vannahme, C., S. Gosling, M. Paulsson, P. Maurer, and U. Hartmann, 2003 Characterization of SMOC-2, a modular extracellular calcium-binding protein. Biochem. J. 373: 805–814. https://doi.org/10.1042/bj20030532

Vowels, J. J., and J. H. Thomas, 1992 Genetic analysis of chemosensory control of dauer formation in Caenorhabditis elegans. Genetics 130: 105–123.

Vuilleumier, R., A. Springhorn, L. Patterson, S. Koidl, M. Hammerschmidt *et al.*, 2010 Control of Dpp morphogen signalling by a secreted feedback regulator. Nat. Cell Biol. 12: 611–617. https://doi.org/10.1038/ncb2064

Wallace, I. M., O. O'Sullivan, D. G. Higgins, and C. Notredame, 2006 M-Coffee: combining multiple sequence alignment methods with T-Coffee. Nucleic Acids Res. 34: 1692–1699. https://doi.org/10.1093/nar/gkl091

Wang, J., R. Tokarz, and C. Savage-Dunn, 2002 The expression of TGFbeta signal transducers in the hypodermis regulates body size in C. elegans. Development 129: 4989–4998.

Wang, L., Z. Liu, H. Shi, and J. Liu, 2017 Two paralogous tetraspanins TSP-12 and TSP-14 function with the ADAM10 metalloprotease SUP-17 to promote BMP signaling in Caenorhabditis elegans. PLoS Genet. 13: e1006568. https://doi.org/10.1371/journal.pgen.1006568

Wang, R. N., J. Green, Z. Wang, Y. Deng, M. Qiao *et al.*, 2014 Bone Morphogenetic Protein (BMP) signaling in development and human diseases. Genes Dis. 1: 87–105. https://doi.org/10.1016/j.gendis.2014.07.005

Wu, M., G. Chen, and Y. P. Li, 2016 TGF-beta and BMP signaling in osteoblast, skeletal development, and bone formation, homeostasis and disease. Bone Res. 4: 16009. https://doi.org/10.1038/boneres.2016.9

Yoshida, S., K. Morita, M. Mochii, and N. Ueno, 2001 Hypodermal expression of Caenorhabditis elegans TGF-beta type I receptor SMA-6 is essential for the growth and maintenance of body length. Dev. Biol. 240: 32–45. https://doi.org/10.1006/dbio.2001.0443

Communicating editor: B. Grant